
Article:
Marini, M, Patacci, M, Felletti, F et al. (2016) Fill to spill stratigraphic evolution of a confined turbidite mini-basin succession, and its likely well bore expression: The Castagnola Fm, NW Italy. Marine and Petroleum Geology, 69. pp. 94-111. ISSN: 0264-8172

https://doi.org/10.1016/j.marpetgeo.2015.10.014

Fill to spill stratigraphic evolution of a confined turbidite mini-basin succession, and its likely well bore expression: the Castagnola Fm, NW Italy

Marini, M. [1*], Patacci, M. [2], Felletti, F.[1], McCaffrey, W. D. [2]

[1] Dipartimento di Scienze della Terra, Università degli Studi di Milano, Via Mangiagalli 34, 20133 Milano, Italy

[2]Institute of Applied Geosciences, School of Earth & Environment, University of Leeds, Leeds, LS2 9JT, UK

* Corresponding author: mattia.marini@unimi.it

Abstract

This study documents the stratigraphic evolution of the Castagnola ponded turbidite mini-basin through analysis of a detailed base-to-top section measured in the central part of the basin. Vertical variations in facies characteristics, thickness ratio of mud cap vs. sandstone of event beds and net/gross are argued to be good proxies for pinpointing the stratigraphic transition from dominantly ponded deposition, where most of the flow is trapped by the confining topography, to a flow-stripping - dominated phase in which an increasingly large part of incoming flows can escape the basin by spilling over the enclosing topography. Thickness statistics of sandstones and mud caps of event beds from the case study show that in the initial stage of turbidite deposition only part of the mud of exceptionally large volume flows escaped the confining topography; as the basin was progressively infilled, nearly all inbound flows were affected by flow stripping, with part of the sand and most of the mud escaping the basin. In the latest recorded stage of deposition the abundance of by-pass features coupled with significant modification of the sandstone bed thickness population suggests that the turbidite system was no longer obstructed frontally, and could step forward onto a healed topography. In order to assess whether the documented trends of turbidite bed characteristics indicative of the 'fill to spill' transition could be recognised from wireline log data alone, synthetic logs were prepared by up-scaling the field data to resolutions typical of borehole geophysical log data. Vertical trends of average bed thickness and net/gross

recognisable in the synthetic data suggest that the transition from ponded to spill-dominated situations should be resolvable in geophysical log data.

Key words: Turbidity Currents, Topographic Confinement, Flow Ponding, Flow Stripping, Fill and Spill, Turbidite Mini-Basin, Borehole logs

1. Introduction

Turbidity current are said to be ponded when seafloor bathymetry fully traps the flow, thereby producing a flat-topped suspension cloud which spreads over the whole basin (Hickson 2000; Toniolo et al. 2006a, b) albeit with strongly layered physical structure (e.g. sediment concentration, grain size and velocity (Patacci et al., 2015). Ponded turbidite systems are common in a range of different geodynamic contexts (e.g. salt-withdrawal mini-basins of continental slopes in passive margins, structurally confined basins of rifted margins and foreland basin systems; Smith 2004) and are well documented from both the subsurface (McGee et al. 1994; Holman and Robertson 1994; Winker 1996; Prather et al. 1998; Lamers and Carmichael, 1999; Argent et al., 2000; Winker and Booth 2000), near seabed analogues (Beauboeuf and Friedman, 2000; Deptuck et al., 2012; Hay, 2012; Prather et al., 2012a, b) and outcrop (Pickering and Hiscott, 1985; Haughton, 1994; 2000; Pickering & Hilton 1998; Sinclair 2000; Tomasso 2001; Sinclair and Tomasso 2002; Amy et al., 2007; Felletti and Bersezio 2010). Flow stripping occurs when the most dilute upper part of a turbidity current suspension cloud is able to escape the basin spilling over the confining topography (Sinclair and Tomasso 2002). Flow stripping can occur either as a transient run-up effect in low relief confined situations (Muck and Underwood 1990), or when large volume, long-lived flows inflate the suspension cloud to the level of a basin sill (Toniolo et al. 2006a, b; Patacci et al., 2015). Whether flow ponding or stripping dominates and how it affects deposition will therefore depend principally upon the physical structure of the inbound turbidity current (e.g. flow thickness, internal stratification in sediment concentration and grain size, velocity, duration and total discharge) and the height of the enclosing topography (Muck and Underwood 1990; Alexander and Morris 1994; Kneller and McCaffrey 1999). These controlling factors may be time-variant due to changes in

sedimentary input and modifications of seafloor bathymetry, including basin infill (Prather et al. 1998; Winker and Booth 2000; Sinclair and Tomasso 2002; Felletti and Bersezio 2010; Sylvester et al. 2015).

Research interest in the architecture of ponded turbidite systems was originally prompted by hydrocarbon discoveries from salt-withdrawal multiple mini-basins of the Gulf of Mexico (e.g. Mars field, Prospect Bullwinkle and Auger Basins) where early workers (Mahaffie, 1993, 1995; Holman and Robertson 1994; McGee et al. 1994; Winker 1996, Prather et al. 1998) identified chains of successive depocentres with a common infill motif. This include a lower dominantly sheet-like sand-prone succession onlapping the basin topography ('ponded facies assemblage' of Prather et al. 1998; *cf.* the 'S' sands of McGee et al. 1994) and an upper shale-prone succession with discontinuous channel sands which locally incise into the older deposits and are physically connected to the next basin down slope ('bypass facies assemblage' of Prather et al. 1998; *cf.* 'R' sands of McGee et al. 1994). The stratigraphic evolution of an ideal ponded depositional sequence described by Prather et al. (1998) from the Auger Basin was later on revisited and integrated with description of component facies by Sinclair and Tomasso (2002) using the Eocene-Oligocene Annot and Taveyannaz sandstones of the western Alpine foreland basin as depositional analogues. These authors reported evidence of stratigraphic transition from a lower sheet-like succession with thick bedded sandstone-mud cap couplets, interpreted elsewhere as ponded turbidites (Van Andel and Komar 1969; Pickering and Hiscott 1985; Haughton 1994, 2000), to an increasingly sand-rich upper section with amalgamated to channelized sandstones which is topped by a condensed unit of fine grained turbidites. The depositional model for 'fill and spill' basins of Sinclair and Tomasso (2002) is four-fold and features i) an initial flow ponding phase during which turbidity currents are fully contained by the confining topography of an upper basin; ii) a flow stripping phase which records the partial surmounting of the confining topography by the uppermost, finer grained fraction of turbidity current depositing its load downstream of it in a lower basin; iii) a flow by-pass phase occurring as the upper basin is filled in and the barrier separating it from the lower basin is healed so to induce either by-pass or abandonment of the upper basin and,

locally, incision through older deposits; iv) a late-stage blanketing phase during which infilling of the lower basin results in reduction of gradients across the whole systems and backfilling where bypass had previously occurred in association with incision. The first two of these stages are amenable to statistical analysis of the distribution of bed thicknesses (Malinverno 1997; Sylvester 2007; Bersezio et al, 2005; 2009; Felletti and Bersezio 2010). Statistical experiments confirm that in a fully ponded scenario the thickness population of turbidite beds is likely to reflect the magnitude distribution of inbound flows (i.e., all the sediment is trapped by the basin topography) whereas when flow stripping occurs (part of the larger flows reaching the sill escapes the basin) thickness statistics are considerably modified (Sinclair and Cowie, 2003; Fig 1).

This study focuses on the confined Castagnola turbidite system (Late Oligocene-Early Miocene), deposited in a mini-basin within the northeast Tertiary Piedmont Basin (Ligurian Alps, Northern Italy). The paper has two main objectives. Firstly, it aims to document the vertical evolution of depositional style of the system during the fill-to-spill transition by assessing changes in key sedimentological parameters (i.e. bed thickness, net to gross, average grain size, bed type proportions and thickness ratio of sandstone to mud cap within single event beds), making a comparison with existing 'fill and spill' depositional models via graphical analytical approaches. Secondly, after up-scaling the outcrop dataset to a resolution comparable to that of wire-line logs the study aims to provide a set of criteria that can be used to interpret subsurface data sets in terms of fill and spill processes. In applied scenarios such analyses can rarely be directly undertaken on core, due to its scarcity.

2. Geological framework of the study area

The Tertiary Piedmont Basin (TPB) of NW Italy was a tectonically mobile, episutural basin developed behind the thrust front of the Mesoalpine belt on the Adria microplate (Mosca et al, 2010; Maino et al 2013). During the Upper Eocene–Miocene, following the continental collision of the European Plate and the Adria microplate, the juxtaposed Alpine and Apennine units were unconformably covered by a complex pattern of orogen-derived sediments that entered the TPB (Figs. 2a). The study area of the present paper lies in the easternmost (Borbera-Curone) sector of

the TPB, in which a 3000-m-thick turbidite succession is developed, ranging in age from late Eocene to early Miocene and comprising four main stratigraphic units: the Monte Piano (Eocene), Ranzano (Late Eocene- Early Oligocene), Rigoroso (Late Oligocene) and Castagnola (upper Late Oligocene-Early Miocene) Formations (Cavanna et al., 1989; Stocchi et al., 1992, Baruffini et al., 1994; Fig 2b). This turbidite succession is at present bounded to the north by a ENE-WSW - striking flower structure associated with the Villalvernia-Varzi Line (VVL), a syn-sedimentary strike slip fault. The Chattian–Aquitanian activity of the VVL (Di Giulio & Galbiati, 1998) induced the folding of the Ranzano and the Rigoroso Formations into a ENE-WSW trending syncline, namely the Castagnola Basin, into which ca. 1000 m-thick succession of turbidites of the Castagnola Formation (Fig. 2b) were deposited during a period of tectonic quiescence. Other turbidite deposits (upper Rigoroso Fm. and Costa Montada Fm., in Andreoni et al., 1981) time-equivalent to the Castagnola Fm have been reported c. 20 km to the WSW in the Arquata Scrivia region, i.e., upstream of the Castagnola Basin, suggesting that the studied turbidites might represent the infill of one of a chain of mini-basins.

2.1. ***The Castagnola Formation***

The Castagnola Fm. comprises three members (Fig. 2b; Cavanna et al., 1989); the older Costa Grande and Arenaceo Members are represented almost exclusively by turbidites whilst the younger Mt. Brugi Marls Member consists of mostly hemipelagic silicified marls with intercalations of thin bedded turbidites. The lower Costa Grande member unconformably overlies the Rigoroso Marls Fm. and reaches a maximum thickness of about 600 m. It comprises basin-wide couplets of tabular turbidite sandstones and mudstones with a sandstone / shale thickness ratio generally more than 1, including several key beds (*Kb a-f* in Fig. 2b) that can be easily traced laterally in the field providing a robust correlation framework across the basin (Cavanna et al., 1989). The overall sheet-like architecture of the Costa Grande Mb. (Fig. 3) has been interpreted to record deposition in a small confined basin from turbidity currents of large volume with respect to the confining bathymetry (Table 1; Cavanna et al., 1989; Stocchi et al., 1992, Baruffini et al. 1994). In addition, petrographic data by Cibin et al. (2003) document the interbedding of lithoarenitic and arkosic sandstones suggesting at least two primary sedimentary sources for the Costagrande Mb.

turbidites. The middle Arenaceo Member is approximately 200 m thick and comprises medium to thick-bedded turbidite sandstones that are typically much thicker than the overlying mud caps (Baruffini et al., 1994) and show a lower lateral continuity with respect to those of the older Costa Grande Member (Table 1). Based on stratal patterns and component facies, the Arenaceo Member has been interpreted as representing depositional lobes of a larger turbidite fan (Andreoni et al., 1981). The overall stacking pattern of these two members forms a coarsening- and thickening-upward trend resulting from an upward increase in the sandstone/shale ratio (Fig. 3). The Mt. Brugi Marls Member, above, has a minimum thickness of c. 160 m and is dominantly composed of decametre-thick packages of thin bedded turbidites; it has been interpreted as the product of deposition in a basin plain environment (Andreoni et al., 1981).

2.2. ***Basin morphology and palaeocurrent trends***

The deposition of the Castagnola Fm. took place in the structural depression forming southward of the Villalvernia-Varzi Line (VVL; Mutti, 1992; Baruffini et al., 1994; Di Giulio & Galbiati, 1998). The long axis of this basin was oriented ENE–WSW, approximately parallel to the strike of the VVL. At the onset of turbidite deposition, basin geometry exerted a pronounced control on shape, component facies and stratal patterns of the turbidite deposits. However, as argued below, the Castagnola Basin likely evolved into a more areally extensive depocentre due to progressive turbidite infill.

Costa Grande Mb.

Owing to well-exposed onlap terminations and mapping of key megabeds (Cavanna et al, 1989), the morphology of the Castagnola Basin at the onset of the deposition of the Costa Grande Mb. can be reconstructed as broadly bowl-shaped, with an estimated length and width of approximately 4 and 2 km, respectively. The initial sheet-like architecture of the younger Costa Grande Mb. (Stocchi et al 1992, Baruffini et al., 1994), has been recently confirmed through detailed bed by bed correlations by Southern et al. (2015) in the stratigraphic interval between *Key beds b* and *c* (Fig. 3). The onlap of the Costa Grande Mb. turbidites onto the northern and north western basin

margin (namely, the bathymetry associated with the VVL flower structure) is represented by an abrupt pinch-out of sandstones ('abrupt onlap' of Smith and Joseph, 2004; type 1 onlap of Sinclair, 2000 and the 'infill geometry' of Hurst et al., 1999) defining an initial slope base trajectory of 11° (Baruffini et al., 1994). Conversely, the southern-south-eastern terminations of the Costa Grande Mb. turbidites consist of pinching and shaling out of turbidite beds (Felletti, 2002), thereby giving rise to an aggradational onlap (*sensu* Smith and Joseph, 2014; type 3 or 'apparent' onlap of Sinclair, 2000) with an average trajectory of less than 5°. The observed turbidite terminations styles and the position of the last documented onlap (i.e. *Key bed d* in Figs. 2b and 3) suggest that during the deposition of the Costa Grande Mb. the size of the Castagnola Basin might have increased up to a minimum of 6x4 km (length x width) due to climbing of onlaps onto basinal slopes.

In the Costa Grande Mb. sole marks indicate well focused NNW to NNE-directed inbound flows, consistent with local sourcing of turbidity currents from the S-SE, together with evidence for flow re-direction parallel to the WSW-ENE – trending basin axis, whereas SW to W-directed palaeocurrents derived from ripples suggest, as described elsewhere (Kneller et al., 1991; Haughton, 1994; McCaffrey and Kneller 2001; Smith, 2004), reflection of the most dilute part of turbidity currents off the northern and eastern bounding slopes (Fig. 3; see also Stocchi et al., 1992; Baruffini et al., 1994; Southern et al., 2015).

Arenaceo and Mt. Brugi Marls Mb.

Due to erosion and uplift to the north of the Villarvernia tectonic line, no lateral terminations of the Arenaceo and the Mt. Brugi Marls Mbs. are preserved (Figs. 2b and 3), which makes it difficult to reconstruct the size and morphology of the Castagnola Basin at the time of their deposition. However, based on the geometry of basinal slopes of the Costa Grande Mb., it can be assumed that the basin area exceeded 24 km^2 (6 km length x 4 km width), which is in agreement with a relatively less focused paleocurrent pattern (Fig. 3) compared to that of the Costa Grande Mb.

3. Methodology

This study is based on detailed sedimentological logging of an 870 m-thick section through the entirety of the Costa Grande and Arenaceo Members of the Castagnola Fm. The section was logged in the south-central part of the Castagnola Basin (locality 2 in Fig. 2b), except for an interval in the middle part of the Arenaceo Mb., which due to poor exposure could only be logged 2 km to the west (locality 1 in Fig. 2b). A second control section was logged in the eastern part of the basin (locality 5 in Fig. 2b) to validate thickness measurements. Logging was performed using a Jacob staff instrumented with an integrated laser pointer which allowed thicknesses to be measured to an accuracy better than 1 cm.

The log data were compiled into a database. For each bed, these included thickness, stratigraphic height of base and top, lithology (i.e. sandstone vs. mudstone), bed type (see Section 4.1), average basal grain size and palaeocurrent type and direction. The grain size was measured using a grain-size comparator, devoting particular care to differentiation of very fine sand and mud. Rare amalgamated beds were measured as individual layers, but with note made of grain-size steps associated with amalgamation surfaces. Turbidite mudstones were differentiated from hemipelagites based on their markedly darker weathering colour, high content of micaceous minerals, weak to no reaction to hydrochloric acid (HCl) and lack of microforaminiferal fauna which are abundant and well preserved in the few hemipelagic beds present in the studied section. This data set allowed a set of secondary parameters to be derived that potentially give insight into the ponding process, such as sandstone to mudstone ratio (with and without hemipelagite), average grain size and bed thickness. Histograms and exceedance probability plots of bed thickness were employed to contrast different stratigraphic intervals of the studied section and to compare their thickness populations with experimental statistical distributions describing flow ponding vs. flow stripping effects (Fig. 1), as modelled by Sinclair and Cowie (2003).

Finally, in order to test the feasibility of assessing confinement state from less detailed data sets, such as those derived from open-hole geophysical logging, some of the stratigraphic parameters and statistics were re-computed on a synthetic data set obtained via up-scaling the field data set. The up-scaling procedure is detailed below in Section 3.1.

3.1. ***Up-scaling of field data to resolution of routinely acquired wire-line logs***

As reproducing a replica of any specific geophysical log was beyond the scope of this paper, an up-scaling procedure was adopted that was aimed solely at reducing the resolution of the field data set to that of synthetic lithology curves such those derived from interpretation of geophysical logs routinely acquired in a well bore (e.g. gamma ray, neutron-density and resistivity logs, see Table 2). The sedimentological log was thus re-sampled at steps at a constant spacing of 25, 50 and 100 cm, extracting a lithology indicator value (1 for sandstone and 0 for mudstone) at each step, alongside stratigraphic height. After extraction, successive readings yielding the same indicator values were aggregated in order to obtain synthetic lithology logs of different vertical resolution (i.e. 25, 50 and 100 cm). This approach simulates a condition where combined interpretation of geophysical logs from a well bore is successful in determining the dominant lithology (i.e. sandstone and mudstone) for each reading. Up-scaled bed thicknesses were extracted from these synthetic lithology logs in order to recalculate bed thickness statistics and to compare them with the full resolution field data set.

4. Results

4.1. ***Bed types***

Five main types of event bed were identified based on grain size, thickness and sedimentary facies associations and named, when applicable, after the nomenclature of Southern et al. (2015).

Type A beds

This bed type includes very thick beds and megabeds (thickness range 2 to 10m) comprising a lower division several dm thick of medium-coarse, normally-graded sandstones with a range of crude to planar-parallel laminations followed by a very thick portion of massive or dewatered sandstones. Thereafter these massive sandstones alternate repeatedly and over thickness of few dm with parallel-laminated sandstones before grading upward into a thick uppermost division of silty-sandstones. In the fine-grained upper interval of Type A beds repeated normal grading (Fig. 4a) and wavy, hummocky-like laminations are common, while well-developed ripple-drift laminations are missing. Moreover, Type A beds are always topped by very thick mud cap which can exceed the thickness of the underlying sand (Fig 5). Typically they have a basin-wide distribution and sheet-form geometry (see for example *Key beds a-d* and *f* in Figs 3 and 6).

Interpretation

The normal grading and crude to parallel lamination of the basal part of type A beds indicates initial deposition from a turbulent suspension and traction in an upper flow regime from the overriding flow. The upward transition to massive sandstone records suppression of traction following a sudden increase in the suspended sediment fall-out rate (Dorrell and Hogg 2012), which possibly reflects the establishment of ponded conditions within the suspension cloud. Repetitions of massive-parallel laminated couplets suggest in turn that the stability conditions of parallel lamination is transiently and cyclically met due to pulsating conditions within the flow (e.g. flow velocity and rate of sediment fall-out from above), possibly due to propagation of internal waves (Patacci et al., 2015). Lastly, the absence of a silty-sandstone division of unidirectional sedimentary structure (e.g. ripple drift lamination) in the upper sections in favour of repeated normal grading and wavy to hummocky–like laminations would suggest that pulsating or even oscillatory flow conditions (Tinterri 2011) lasted to the final stage of sedimentation, prior to deposition of the thick ponded mud cap (Pickering and Hiscott, 1985; Haughton 1994, 2000). The vertical sequence of sedimentary structures along with the average thickness of both the sandstone and the mud cap of type A beds suggest deposition from large volume turbidity currents

ponded by the enclosing topography (Lamb et al., 2004; Toniolo et al., 2006a, b; Patacci et al., 2015).

Type B beds

This bed type includes thick to very thick normally graded beds (thickness range from c. 0.5 m to 4 m) that typically comprises a thick lower division of fine to medium parallel-laminated sandstone passing upward into an upper division of fine to very fine silty-sandstones with ripple drift laminations capped by a relatively thick mud cap (Figs 4c and 5). The fine grained tops of these bed types can contain bedform sets with opposite palaeocurrent directions that pass upward to wavy and hummocky-like laminations (Fig. 4b). Mud caps of this bed type are generally thicker than the co-genetic underlying sandstone.

Interpretation

The thickness of the lower parallel-laminated interval along with the average overall thickness of type B beds suggest persistence of deposition in the upper flow regime. The presence of multiple bedform sets with opposite palaeocurrent direction followed upward by wavy and hummocky-like laminations indicate reflection of the upper and more dilute part of parent flows off the laterally confining slopes (Kneller et al., 1991; Haughton, 1994; McCaffrey and Kneller 2001; Smith, 2014) and establishment of a late phase of oscillatory flow conditions (Tinterri 2011), respectively. These features suggest that type B beds were deposited from flows of intermediate volume developing a ponded character in response to containment by the confining topography.

Type B' beds

Type B' beds comprise a lower division of ungraded medium-coarse sandstone with massive appearance and sharp top capped by a very thin division of very fine silty sandstones with ripple drift laminations. Locally, Type B' beds can locally have cm-deep basal scours with lags of fine

pebbles indicating shallow erosion of the substrate and be welded to form packages of amalgamated beds (Fig. 4d). Typically, type B' beds are much thinner than type B beds (thickness range 0.40 to 1.6 m) and are capped by cm to few dm-thick mud caps (Figs 4c and 4g).

Interpretation

The lower sharp-topped structureless sandstone followed upward by a rippled division and a mud cap of reduced thickness with respect to other turbidite beds of the study interval suggest rapid sedimentation of the coarser-grained load from unconfined parent flows that were partially by-passing. Type B' beds are interpreted as the product of deposition in the intermediate to proximal regions of an unconfined turbidite fan (Mutti and Normark, 1991).

Type C beds

Type C beds are thick to very thick beds (thickness range from c. 0.6 m to 3.5 m) generally showing a tripartite structure consisting of a base and top intervals similar to the *Ta-b* and *Tc-d* divisions of the *Bouma* sequence, respectively, sandwiching a middle division of highly variable internal organization. The latter may consist of a package of m-scale folded to sheared rafts of heterolithic sediments floating in a scarce matrix, a relatively clean sandstone charged with large mud and sandstone rafts or even a dirty-looking, mud-rich sandstone with small rounded mud clasts. Southern et al., (2015) describe in detail the character and lateral variability of these beds in the Castagnola basin.

Interpretation

Type C beds are interpreted to represent different stages of flow transformation of turbidity currents into hybrid flows, namely flows in the form of a frontal turbidity current and a lagging co-genetic debris flow (Haughton et al., 2003; Haughton et al., 2009; Talling, 2013; Southern et al., 2015).

Type D beds

This bed type includes beds of ripple-drift laminated very fine, silty sandstones several cm to a few dm thick which typically grade upward into a mud cap, whose thickness may range from a few cm to several dm. In the Costa Grande Member, these beds often comprise two main bedform sets separated by a lag of plant fragments, with incoming NE palaeocurrents in the lower set and reverse palaeocurrents in the upper set.

Interpretation

Type D beds are interpreted as the product of deposition from highly dilute waning flows which despite their relatively small volume were able to interact with bounding topography. Disperse palaeocurrent directions represent the result of deflection and/or reflected of the incoming flows from the confining topography.

4.2. ***Vertical trends in the logged section***

Based on vertical trends in sandstone and mud caps thickness, bed type proportions, grain size and net/gross the studied section of the Castagnola Fm. can be subdivided into the three main units (Fig. 6).

Unit 1

This unit is 570 m thick and represents more than a half of the total thickness of the studied section. The basal part of Unit 1 is represented by a 20m-thick mud-rich(net/gross <20%) thin-bedded interval which sits unconformably upon the Rigoroso Fm. and comprises exclusively type D beds. The thickness of these beds varies in range from a few cms to a few tens of cms and their mud caps are thinner than equivalent beds from the upper section. The beds pinch out gradually toward the south, where they onlap the underlying Rigoroso Fm. marls 100–150 m away from the measured section. Above this thin bedded package (stratigraphic height 50-100m), average thickness of beds and mud caps increase as a result of the first occurrence of Type B and C Beds.

From *Key bed a* (of Stocchi et al., 1992; *Key bed 2* of Cavanna et al, 1989) onwards, the stratigraphy of Unit 1 is punctuated by the recurrence of Type A megabeds. This results in cyclic changes in bed type proportions and fluctuation in both average and standard deviation of sandstone bed and mud cap thickness. The uppermost 50 m of Unit 1 are dominated by closely spaced Type C beds which result in a localized increase in average and standard deviation of thickness of sandstone beds as well as net/gross and grain size and a steady decrease in average and standard deviation of mud cap thickness.

Bed type proportions indicate that bed types A and B represent the main constituents of Unit 1, followed by beds of Type D, which are relatively more common in the lower section of the unit, and then Type C beds, that recur mostly within mud-rich intervals and become more frequent above *Key bed c* (of Stocchi et al., 1992; *Key bed 3* of Cavanna et al, 1989). Although net/gross of Unit 1 is highly variable with peaks (≈0.2-0.3) and lows (≈0.05-0.1) which broadly correspond to the position of Type A megabeds and thin-bedded intervals, respectively, an overall upward increase in sand content and grain size can be observed (Fig. 6). Also it should be noted that, with the exception of the type C-dominated interval, the average thickness of mud caps is higher than that of sandstone beds.

Unit 2

Above the type C-dominated interval of the uppermost part of Unit 1, net/gross and grain size drop to values comparable to that of the upper half of Unit 1 prior to rapidly increasing again above *Key bed f*. This trend reflects the continuing upward reduction of average thickness of mud caps (Fig. 6) which, starting from the middle of the unit, is paralleled by a gradual increase in average thickness of closely packed sandstone beds. In terms of bed type proportions, *Key bed f* is the only type A bed present in the unit, whereas type B beds are numerous and more abundant than in the underlying Unit 1. Finally, type C beds represent an important fraction of the total thickness and, as already seen in Unit 1, commonly occur within mud-rich, thin bedded intervals (Fig. 6).

Unit 3

Unit 3 is typified by an upward increase in thickness and standard deviation of sandstone beds and a decrease in thickness and standard deviation of mud caps. These trends are paralleled by an initial increase in thickness proportion of type C beds, which disappear around the middle of the unit, and an upward decrease in proportion of type B beds which, starting from stratigraphic height 700 m, disappear in favour of type B' beds. It should be noted that type A megabeds (interpreted to reflect 'ponded' conditions) are not present in this unit.

4.3. ***Sandstone bed vs. mud cap thickness***

The relationship between sandstone and mud cap thicknesses for individual event beds is shown in log-log scatter plots for different bed types (Fig. 7), subdivided by host unit. Linear fitting of data points within each class was undertaken, bearing in mind that i) the initial grain size distribution (and hence, the initial amount of mud) may vary from flow to flow; ii) the use of interpretative categories such as bed types and stratigraphic units may hide the transitional character of sedimentary processes; iii) overestimation of mud cap thickness may occur when two or more mud caps are measured as one, due to a thin or absent coarser basal layer; iv) binning errors may arise when assigning integer cm thicknesses to thinner beds. Considerations iii and iv principally apply to the thinner (less than 1 dm-thick) Type D beds which were therefore not represented on Fig 6.

If we consider bed types A, B and B' (Fig.6a), the relatively high coefficient of determination R^2=0.8 (i.e. the square of the Pearson correlation coefficient) of Unit 1 indicates a significant correlation between the thickness of mud caps and that of the underlying sandstone in this unit. The correlation becomes weaker (R^2=0.5) to nearly absent (R^2=0.01) in the younger Units 2 and 3, respectively. In addition, except for two of the thicker beds (*Key beds c* and *d*), type A, B and B' event beds in Unit 1 have mud caps that are thicker than the underlying sandstone and tend to cluster above those of Unit 2, whereas event beds of Unit 3 always have mud cap to sandstone thickness ratios lower than 1. Conversely, type C beds (Fig. 7b), show a low coefficient of determination, R^2, in all units. This can be interpreted to reflect the inherent complexity of hybrid

flows, which is thought to involve *en-route* entrainment of significant amounts of sediment (see Southern et al, 2015). Nevertheless, it is significant that data points of Unit 1 tend to plot above those of Unit 2 indicating thicker mud caps whereas those of Unit 3 occupy the lowermost half of the graphs (Fig.6b). It is interesting to note that if we consider the mud cap to sandstone thickness ratio vs. the total thickness of event beds (Fig. 8) a weak inverse relationship is seen in data points of Unit 1 and 2, which suggests that the thickness proportion of mud cap reduces for increasing magnitude of parent turbidity currents.

The stratigraphic variability of mud cap to sandstone thickness ratio and its relationship with bed type is shown in Fig 8. Regardless of bed type the thickness proportion of event bed mud caps progressively decreases above stratigraphic height c. 450 m. On average type B' beds show the lowest ratio of mud caps to sandstone thickness for each event bed, followed by beds of Type C, then Type A and finally Type B.

4.4. ***Bed thickness statistics***

Histograms of thickness of type A, B and B' beds indicate a reduction in the relative abundance of sandstone beds thicker than ca. 4 m in favour of thinner beds moving upward from Unit 1 to Unit 3 (Fig. 10a, see also maximum bed thickness values in Table 4). Conversely, the statistical distribution of thickness of the sandstone portion of type D beds remains the same throughout the studied interval (Fig. 10b). If we consider mud caps of whichever bed type, it can be noted that starting from Unit 2 mud caps thicker than 2 m ca. disappear (Figs. 10a and b and Table 3). Furthermore, mud caps thickness of beds of Type A, B and B' decrease in maximum, mean and standard deviation from Unit 1 to Unit 3 (Fig. 10a and Table 3).

The thickness populations of both the sandstone and the mudstone components of event beds are plotted as number of entries thicker than thickness H against H (i.e., as log-log exceedance plots) for Units 1-3 in Figs. 11a, b and c, respectively. This representation of the bed thickness distribution data enables comparison with those modelled by Sinclair and Cowie (2003). The

thickness of sandstone beds from Unit 1 (Fig. 11a) plots as a nearly linear trend similarly to the that modelled by Sinclair and Cowie (2003) for ponded turbidite beds (Fig. 1), suggesting that nearly all of the sand was trapped by basin topography in this Unit. Conversely, the sandstones beds from Unit 2 and 3 (Fig. 11b and c, respectively) define convex-upward curves that resemble the experimental distributions of turbidites subject to flow stripping of Sinclair and Cowie (2003) as well as those reported in the literature from non-ponded, open ended turbidite systems (see for example Talling, 2001). However, a significant change of gradient of the exceedance plot for sandstone thickness in Unit 2 occurs at a thickness of c. 125 cm (i.e. within the thickness range of type B beds). Above this point, the thickness of the sandstone beds is lower than one would expect based on the distribution of the thin-bedded part of the population. This feature of the sandstone bed population of Unit 2 can be interpreted to relate to a threshold of turbidity current magnitude over which stripping affects also the sandy part of the flow leading to deposition of sandstone beds that are thinner than in a ponded depocentre.

Considering the mud caps, the statistical populations of Unit 2 and 3 plot as upward convex curves and are 'truncated' at their thick-bedded end (i.e., at around a thickness of 185 cm and 90 cm ca., respectively; see maximum mud cap thickness in Table 3) in a fashion similar to the distribution modelled by Sinclair and Cowie (2003) for flow stripping (Fig. 1). Conversely, the curve of Unit 1 inflects at a thickness of 80 cm ca. (black arrow in Fig. 11a). This point subdivides the dataset into two subpopulations: a thin-bedded population (i.e. beds thinner than 80cm ca.) with the same slope as that of the sandstone bed distribution and a thick-bedded population (beds thicker than 80 cm ca.) with a steeper slope. As seen for sandstone beds of Unit 2, such a change in gradient of the exceedance plot suggests that the thickness of mud caps from the thick-bedded subpopulation is lower than one would expected based on the distribution of the thin-bedded subpopulation alone, and is likely related to stripping of mud in large volume flows.

5. Discussion

The following discussion of the stratigraphic trends observed in the Castagnola Fm relies on the assumption that sediment input was self-similar all over the studied interval in terms of sand to mud ratio. At present, there is no strong evidence to confirm or exclude this assumption, which would require detailed petrographic inquiries into both sandstones and mud caps.

5.1. ***Depositional interpretation of the studied units***

The character and proportion of dominant beds types of Unit 1 (lower Costa Grande Mb. of the Castagnola Fm.) suggest that topographic confinement played a key role in controlling turbidite deposition during this phase. In Unit 1 the thickness of mud caps is generally greater than that of the underlying sandstones which is consistent with the ponding of incoming turbidity currents. However, the variability in mud cap thickness proportion appears related to event bed type (Fig. 7), stratigraphic height (Fig. 8) and total event bed thickness (Fig. 9). In particular, relative mud cap thickness appears to decrease with increasing stratigraphic height and with increasing bed thickness. These relationships suggest that, especially for exceptionally large volume flows, part of the mud-grade sediment escaped the confining topography perhaps during even the earliest deposition of Unit 1 and that stripping of mud became gradually more important with the progress of deposition. However, the similarity between the sandstone bed statistics of Unit 1 and data modelled by Sinclair and Cowie (2003) for ponded turbidites appear to indicate that during deposition of Unit 1 the receiving basin topography could fully trap the sandy part of incoming flows. These observations lead us to interpret Unit 1 as recording deposition under partially ponded conditions for large flows, whereby effectively all of the sand load of incoming flows was trapped by the receiving topography whereas the upper, finer-grained part of suspension cloud underwent at least some flow stripping. Small flows were instead probably fully ponded at the onset of Unit 1 deposition. A similar differential likelihood of ponding of large (and thicker) vs. small (and thinner) flows has been inferred in the Peira Cava outlier of the Annot sandstones (Amy et al. 2007) and demonstrated experimentally (Brunt et al. 2004).

Similarly to the upper part of Unit 1, Unit 2 is characterized by a stratigraphic decrease of the mud cap to sandstone thickness ratio (Fig. 8) which again, is tied to bed type (Fig. 7) and total event bed thickness (Fig. 9) as seen for Unit 1. These relationships suggest an increasingly important impact of flow stripping on finer grained sediments, which is in agreement with the ongoing infilling of the basin. In addition, thickness statistics of sandstone beds indicate a decrease in the number of very thick beds, which is consistent with the data modelled by Sinclair and Cowie (2003) for flow stripping. During this phase part of the sand load of the incoming turbidity currents could likely escape over the confining topography (see experimental work of Brunt et al. 2004). It can be speculated that the inflection point highlighted in Fig. 11b may represent a critical value of sandstone bed thickness relating to a threshold of flow magnitude above which spilling significantly affects the sandy deposits of partially ponded flows. Based on these observations and on the assumption that the sediment input did not change significantly in terms of grain size and sand/mud proportions, Unit 2 is interpreted as recording the onset of flow stripping-dominated conditions in the Castagnola Basin, which may have been relatively shallow. This change involves most of the thickness of incoming turbidity currents, affecting not only the net/gross, but also the sandstone bed thickness.

Lastly, the rapid replacement of 'ponded' A-B bed types by type B' *Bouma*-like turbidites with sharp tops and the disappearance of multiple palaeocurrents in rippled beds in Unit 3 are taken to indicate switching from deposition under partially ponded conditions to deposition within a virtually open-ended basin. The associated upward increase of net/gross and grain size, alongside thickening of sandstone beds and thinning of mud caps (Fig. 6) can be interpreted as the result of forestepping of the Castagnola turbidite systems onto the healed topography where most of the finer grained fraction of incoming flows by-passed downstream. In this interpretation Unit 3 would represent an example of perched apron (*sensu* Prather et al., 2012).

Although there is no direct evidence either of younger turbidites downstream of the study area or development of a later phase of incision cutting into the ponded basin fill ('Flow bypass by incision'

of Sinclair and Tomasso, 2002), outcrop constraints do not permit these possibilities to be ruled out. However, deposition of hemipelagites and thin bedded fine grained turbidites of the Mt. Brugi Marls Mb. found above Unit 3, is consistent with establishment of a low energy setting, such as a healed slope, lateral to a bypass channel ('Flow bypass by abandonment' of Sinclair and Tomasso, 2002).

5.2. ***Full resolution vs. up-scaled data***

In Fig. 12, the full resolution sedimentological log measured in the field is compared with synthetic sand/mud logs at different vertical resolutions (see paragraph 3.1 for methodology) in an attempt to replicate lithology curves that could be obtained from the interpretation of geophysical well logs.

Prior to making this comparison, it is useful to consider the simple case of a succession of interbedded sandstone and mudstone beds of thickness greater than that of the vertical resolution and with no major stratigraphic trends in sand/mud and bed thickness. In this case, the probability at each sampling step of picking a bed of either sandstone or mudstones is directly related to relative abundance of that lithology. However, when one of the two lithologies is consistently subordinate and has average bed thickness smaller than vertical resolution a detection bias should exist toward the most abundant lithology.

In this regard, we can consider the statistics of sandstone and mudstone bed thickness by bed type and stratigraphic unit (Fig. 10) as well as the net/gross of the three units, which suggests that any bias would affect the synthetic lithology curve reconstructed for the three studied units differently. In the mud-rich intervals of Unit 1 and Unit 2 the number of very thin to thin sandstone beds appears to be underestimated, whereas in sand-rich intervals of Unit 3 underestimation occurs for the thinner mud caps (Fig. 12). One obvious drawback of under-detecting thin beds is that in particularly unfavourable conditions, internally-stratified depositional units might be imaged on geophysical logs as lithologically homogenous units, as if they were single depositional events or amalgamated depositional bodies. In addition, as the sampling frequency decreases (Fig. 12, left to right), very thin and thin beds are increasingly under detected which might result in an increased blockiness of the lithology curve.

As a result of such sampling biases, the statistics of bed thicknesses extracted from synthetic lithology logs of different vertical resolution are modified significantly with respect to that of real field data (Fig. 13a). Moving from higher to lower sampling frequency (i.e. from b to d in Fig 12) the proportion of thick and very thick mudstone beds in Unit 1 and Unit 2 and of sandstone beds in Unit 3 increases, while the proportion of the thin bedded fraction of the population decreases. As a result, when the average bed thickness is calculated from the synthetic lithology logs the stratigraphic trends of sandstone and mudstone beds thickness are exaggerated as the vertical resolution is reduced (Fig. 14). Conversely, such a drop in vertical resolution does not affect the net/gross estimations (maximum inaccuracy in order of +/-7%) or its stratigraphic trend significantly. The different sensitivity of average bed thickness and net/gross to sampling frequency reflects the strong influence that the numerous thin beds have on average of bed thickness as opposed to their relatively small cumulative thickness.

Some of the key stratigraphic trends described in paragraph 4.2 can be still discerned with good confidence from the curves of Fig. 14. These are: i) the gradual increase of net/gross from bottom to top of Unit 1, which in the upper part of the unit is coupled to the convergence of average thickness of sandstone and mudstone beds. As discussed in section 4.1.1, this trend would result from flow stripping of the uppermost muddy part of turbidity current suspension clouds; ii) a sharp increase in net/gross which is paralleled by a mild drop in average thickness of sandstone beds and the enduring convergence of averages of thickness of sandstone and mudstone beds. These trends reflect the onset of stripping of part of turbidity currents' sand load and enhanced stripping of mud-grade sediments; iii) the crossing of the curves of average thickness of sandstone and mudstone beds at the boundary between Unit 2 and 3, and iv) the divergence of the same curves over most of the thickness in Unit 3, which records by-pass of fine grained sediments and, it is thought, gradual forestepping of the frontally unobstructed turbidite system. It can be noted that exceedance plots based on up-scaled data become increasingly less diagnostic of the transition from ponding to flow stripping conditions as the vertical resolution decreases, suggesting that bed

thickness statistics cannot be used for this purpose unless lithology logs of high resolution are available.

6. Conclusions

6.1. ***Transition from ponded to flow-stripping-dominated condition in the Castagnola mini-basin***

The stratigraphic trends in facies character, mud cap proportion within event beds and net/gross from a base-to-top section through the sheet-like turbidite systems of the Castagnola Fm. suggest transition from an initial dominantly ponded small basin (Unit 1) to a virtually unconfined basin (Unit 3) via less confined basin dominated by flow stripping (Unit 2). Such a stratigraphic evolution fits well with the first two stages of the 'fill and spill' depositional model (e.g., Sinclair and Tomasso, 2002) in that as the height of the confining topography is reduced because of sediment infilling the basin, an increasing amount of fine grained sediments escape the basin so that the net/gross increases stratigraphically upwards (see also Amy et al., 2007 and Brunt et al., 2004). Although there is not direct evidence of a further depocentre downstream, deposition of hemipelagites with intercalations of thin bedded turbidites in the Brugi Marls Mb. may indicate deposition on a healed slope ('flow bypass by abandonment' *sensu* Siclair and Tomasso 2002) coeval with flow in an (unobserved) bypass channel feeding another depocentre downstream.

When the mud cap proportion within event beds of Unit 1 and 2 is assessed in more detail, an inverse correlation with total event bed thickness emerges, with the lowest values associated with most of type A beds and the thickest type B beds (e.g. *Key beds a-d* and *f* and *Key bed e*, respectively in Figs 8 and 9). These observations imply that stripping of mud not only increased gradually as a result of basin infill, but was enhanced in the event of exceptionally large turbidity currents (Muck and Underwood, 1990; Brunt et al., 2004; Amy et al., 2007) and could take place even during the earliest deposition in the Castagnola Basin; sandstone thicknesses from the same unit are in agreement with the model of Sinclair and Cowie (2003) for ponded turbidites. In

addition, if the range of inbound flows remains the same throughout deposition of the studied section, the lack of a thick-bedded tail in the mud cap populations of Unit 2 and 3 entails a dramatic increase of stripping of the mud which is paralleled with a significant departure from the bed thickness statistical distribution of the older Unit 1. In Unit 2 this departure consists in a sudden decrease in the slope of the exceedance plot across a thickness threshold that must scale to a critical flow magnitude above which flow stripping also affected the sandy part of the turbidity currents. The exceedance plot of sandstone beds of Unit 3 are similar to published data from non-ponded turbidite systems (see for example Talling, 2001).

In summary, these observations confirm: i) the strongly transitional nature of the passage from an almost fully-ponded condition (e.g. Unit 1: thick mudcaps), via a flow stripping-dominated condition (e.g. Unit 2: thinner mudcaps and a deficiency in thicker beds) to an unconfined condition (e.g., Unit 3; yet thinner mudcaps, and an absence of outsized beds); ii) the ability of the muddy component of large volume flows to undergo partial flow stripping even in the initial phase of deposition within a confined-ponded basin; iii) the ability of part of the sand of large volume flows to undergo stripping when the height of the confining topography is in the order of a few tens of metres (Unit 2); iv) the non-exclusiveness of ponding and flow stripping processes which, as early noted by Winker and Booth (2000), can occur at any time during the infill history of a confined basin depending on the height of the confining topography with respect to thickness of the incoming flows.

6.2. ***How can the transition from ponded to flow stripping-dominated conditions be recognized in wellbore geophysical logs?***

Scrutiny of up-scaled data suggests that the level of detail of bed thickness information that could be extracted from a synthetic lithology curve, such as that obtained from routine geophysical logging of a wellbore, might be not sufficiently detailed to pursue sand- or mud cap exceedance plot analysis, as applied to the Castagnola field dataset (depending on the resolution of the logging tool and the characteristic thicknesses of the sand- and mudstones in the logged interval).

Nevertheless, even when the vertical resolution of lithology/bed thickness information drops significantly, the combination of vertical trends in parameters such as average thickness of sandstone and mudstone beds and net/gross can help place the ponded to non-ponded transition. It follows that assessment of the ponding condition can be applied to exploration targets where only routine geophysical logging in a single exploration wellbore is available and refined with local details from core and image logs.

Acknowledgments

This researchwas funded by the Turbidites Research Group industry consortium (Anadarko, BG Group, BP, ConocoPhillips, Dana Petroleum, Nexen, OMV, Petronas, Statoil, Tullow Oil and Woodside). We gratefully acknowledge Bradford E. Prather and Ru Smith for valuable reviews which helped improving the clarity of the manuscript.

Figure and Table captions

Table 1. Some characteristics of the Castagnola Fm. members compiled from the following literature: (a)=Andreoni et al.(1981); (b)=Stocchi et al. (1992); (c)=Baruffini et al.(1994)

Table 2. Wire-line geophysical measurement tools most commonly employed singularly or in combination to predict lithology and their approximate vertical resolution, from ODP (2014)

Table 3. Main characteristics and process interpretation of turbidite bed types of the Castagnola Fm.

Table 4. Thickness statistics of sandstone beds and mudstone caps per stratigraphic unit for bed types A-B-B'.

Figure 1. Dynamics of (a) flow ponding and (b) flow stripping (left-hand side, modified after Sinclair and Tomasso, 2002) are paralleled with simulated statistical distributions of sandstone bed thickness (plotted as Log of number of beds thicker than thickness H vs. Log H) that would result from the two processes starting from a input signal with power law distribution of exponent β=-1.4 (right-hand side, modified after Sinclair and Cowie 2003).

Figure 2. Simplified geological maps of (a) the Tertiary Piedmont Basin (modified after Andreoni et al., 1981) and (b) the Castagnola Basin. In (b) position of the correlation panel of Fig. 3 is shown together with the onlap terminations of the marker beds onto the pre-turbidite substrate (modified after Stocchi et al., 1992)

Figure 3. Strike-section correlation panel (see Fig. 1b for location) from Stocchi et al. (1992) integrated with new data from the Arenaceo Member and rose diagrams of palaeocurrents (dark grey=grooves; light grey=ripples) from Unit 1, 2 and 3. Note the overall tabular geometry of the Costa Grande Mb. and bed terminations against the basin margins. The red rectangle shows the position of the measured log of Fig.6.

Figure 4. Details of some of the bed types and bedding styles of the Castagnola Fm. (a) cyclical normal grading marked by lags of plant fragments in the upper section of a Type A bed; (b) vertical sequence of sedimentary structures from planar-parallel lamination (p-pl) to ripple-drift lamination (r-dl), hummocky-like cross lamination (hc-ll) and wavy laminations (wl) within a Type B bed; (c) the onlap of the Costagrande Mb. onto the Rigoroso Marls Fm. at the north-eastern basin margin

showing the stratal pattern of ponded beds with thick mud caps; (d) amalgamation of Type B' beds in the Arenaceo Mb. showing the reduced thickness of both the fine grained top (fgt) and the intervening mud cap (mc) resulting from partial erosion and significant by-pass; (e) Type B' sandstone beds of the Arenaceo Mb. Note the reduced thickness of mud caps compared to those of the Costagrande Mb. (c of this figure).

Figure 5. Thickness percent histograms of sandstones of event beds per bed types. For bed types A-B-B', empty bars are thickness percent histograms of mud caps.

Figure 6. Stratigraphic-sedimentological log of the measured section with bed type thickness proportions (as percentage, calculated over steps of 25m; left-hand side), average thickness of sandstone beds (red) and mudstone beds (grey), basal grain size (green) and net/gross (dark green) calculated over steps of 50m. Dotted lines of same colours are standard deviations (as absolute values).

Figure 7. Log-Log scatter plots of sandstone vs. mud cap thickness (m) of individual event beds, subdivided by stratigraphic unit. (a) Type A, B and B' beds, with the Key beds (*Kb*, see Fig. 6) identified and (b) Type C beds. Linear regression best fit lines are reported along with their R^2coefficients.

Figure 8. Log-Log scatter plots of event bed thickness (m) against mud cap thickness proportion for individual event beds of type A, B and B', grouped by stratigraphic unit. Note the weak decrease of mud cap proportion in very thick key beds (*Kb a-f*, see Fig. 6 for stratigraphic location). The dashed line indicates 1:1 mud cap to sandstone proportion.

Figure 9. Scatter plot of thickness ratios of mud cap to sandstone bed (logarithmic scale) vs. stratigraphic height in m (linear scale). Note the position of data points with respect to the 1:1 thickness ratio reference line. Stratigraphic location of the key beds (*Kb a-f*) is indicated in Fig. 6.

Figure 10. Percent histograms of thickness of sandstone (full colour, grey) for type (a) A-B-B' and (b) type D beds per stratigraphic unit. In (a) dashed lines are percent histograms of thickness of mud caps.

Figure 11. Log-log exceedance probability plots of sandstone (grey dots) and mud caps (empty circles) thickness of Type A, B and B' per stratigraphic units A (top), 3 (middle) and C (bottom). Note the similarities with experimental results of Sinclair and Cowie (2003) and Fig 3. The black arrows highlight breaks in the slope of the distributions that may possibly relate to the threshold of parent flow magnitudes over which sediment stripping occurs. Note that Type B' beds are not present in units 1 and 2 whereas Type A beds are absent in Unit 3.

Figure 12. Details of the sedimentological log contrasting the stratal patterns (left) of Unit 1 (bottom), Unit 2 (middle) and Unit 3 (top) with idealized sand/mud lithology curves obtained re-sampling the actual field data at steps of 25, 50 and 100 cm.

Figure 13. Histograms of thickness of sandstone beds (full colour, grey) and mud caps (dashed line) from (a) the field data set and the up-scaled datasets with re-sampling steps of 25 cm (b), 50 cm (c) and 100 cm (d).

Figure 14. Curves of average thickness of sandstone and mudstone beds from the actual field data (continuous lines, lower axis) and synthetic lithology logs (dashed lines, upper axis) with vertical resolution of 25 cm (left), 50cm (middle) and 100cm (right). The dark green dotted lines indicate the percent difference (top of upper axis) between net/gross calculated from synthetic lithology logs and that calculated from the actual field data.

References

Amy, L. A., Kneller, B. C., and McCaffrey, W. D., 2007. Facies architecture of the Grès de Peïra Cava, SE France: landward stacking patterns in ponded turbiditic basins. Journal of the Geological Society,164, 143-162. doi: 10.1144/0016-76492005-019.

Andreoni, G., Galbiati, B., Maccabruni, A. and Vercesi, P.L., 1981. Stratigrafia e paleogeografia deidepositi oligocenici sup. – miocenici inf. nell'estremita` orientale del bacino ligure-piemontese. Riv. Ital. Paleontol. Stratigr., 87, 245– 282.

Alexander, J. and Morris, S., 1994. Observations on experimental, non channelized, high-concentration turbidity currents and variations in deposits around obstacles. Journal of Sedimentary Research, Section A: Sedimentary Petrology and Processes 64(4): 899-909.

Argent, J.D., Stewart, S.A., and Underhill, J.R., 2000, Controls on the Lower Cretaceous Punt Sandstone Member, a massive deep-water clastic deposystem, Inner Moray Firth, U.K. North Sea: Petroleum Geoscience, v. 6, p. 275–285.

Baruffini, L., Cavalli, C. & Papani, L., 1994. Detailed stratal correlation and stacking patterns of the Gremiasco and lower Castagnola turbidite systems, Tertiary Piedmont Basin, northwestern Italy. InP. Weimer, A. H. Bouma& B. F. Perkins (Eds.), 15th Annual Research Conference Submarine fansand Turbidite Systems (pp. 9-21). GCSSEPM Foundation.

Beaubouef, R.T., Friedmann, S.J., 2000. High resolution seismic/sequence stratigraphic framework for the evolution of Pleistocene intra slope basins, western Gulf of Mexico: Depositional models and reservoir analogs. In: Weimer, P., Slatt, R.M., Coleman, J., Rossen, N.C., Nelson, H., Bouma, A.H., Styzen, M.J., Lawrence, D.T. (Eds.), Deep-water reservoirs of the world.GCSSEPM Foundation 20th Annual Research Conference 40 Deep-Water Reservoirs of the World, December 3–6, 2000, pp. 40-60.

Bersezio R., Felletti F. & Micucci L., 2005. Statistical analysis of stratal patterns and facies changes at the terminations of a 'turbiditic' sandbody: the Oligocene Cengio Unit (Tertiary Piedmont Basin). GeoActa. Vol.4, pp. 83-104

Bersezio R., Felletti, F.,Riva R. & Micucci L., 2009. – Bed thickness and facies trends of turbiditic sandstone bodies. Unravelling the effects of basin confinement, depositional processes and modes of sediment supply. In Kneller, B., Martinsen, O.J., and McCaffrey, B., eds., External Controls on Deep-Water Depositional Systems: SEPM Special Publication 92, p. 303-321.

Booth, J.R., Duvernay, A.E., Pfeiffer, D.S., and Styzen, M.J., 2000, Sequence stratigraphic framework, depositional models, and stacking patterns of ponded and slope fan systems in the Auger Basin: central Gulf of Mexico slope, in Weimer, P., Slatt, R.M., Coleman, J., Rosen, N.C., Nelson, H., Bouma, A.H., Styzen, M.J., and Lawrence, D.T., eds., Deep-Water Reservoirs of the World: Gulf Coast Section SEPM Foundation, 20th Annual Bob F. Perkins Research Conference, p. 82–103.

Brunt, R.L., McCaffrey, W.D., Kneller, B.C., 2004. Experimental modelling of the spatial distribution of grain size developed in a fill-and-spill mini-basin setting. Journal of Sedimentary Research, 74(3), 438-446. DOI:10.1306/093003740438.

Cavanna, F., Di Giulio, A., Galbiati, B., Mosna, S., Perotti, C. R. & Pieri, M., 1989. Carta geologicadell'estremità orientale del Bacino Terziario Ligure-Piemontese. Atti Ticinesi di Scienze della Terra,32.

Cibin, U., Di Giulio, A., and Martelli, L., 2003. Oligocene-Early Miocene tectonic evolution of the northern Apennines (northwestern Italy) traced through provenance of piggy-back basin fill successions. Special publication – Geological Society of London, 208, 269-288.

Davis, C., Haughton, P.D.W., McCaffrey, W.D., Scott, E., Hogg, N. and Kitching, D., 2009. Character and distribution of hybrid sediment gravity flow deposits from the outer Forties Fan, Palaeocene Central North Sea, UKCS. *Marine and Petroleum Geology* **26** (10): 1919-1939

Deptuck, M.E., Sylvester, Z. & O'Byrne, C.J. (2012) Pleistocene Seascape Evolution above a "Simple" Stepped Slope-Western Niger Delta. In: Application of the Principles of Seismic Geomorphology to Continental-Slope and Base-of-Slope Systems: Case Studies from Seafloor

and near-Seafloor Analogues (Ed. by B. E. Prather, M. E. Deptuck, D. C. Mohrig, B. van Hoorn & R. B. Wynn), Sepm Special Publication 99, 199-222. SEPM (Society for Sedimentary Geology).

Di Giulio, A. &Galbiati, B., 1998.Turbidite record of the motions along a crustal-scale tectonic line:the motions of the Villarvernia-Varzi line during the Oligocene-Miocene (North-Western Italy). In: 15th International Sedimentological Congress, (pp. 293-294). IAS - Universidad de Alicante, Alicante, Spain.

Dorrell, R. M., and A. J. Hogg (2012), Length and time scales of response of sediment suspensions to changing flow conditions, J. Hydraul. Eng., 138(5), 430–439.

Felletti, F., 2004a. Statistical modelling and validation of correlation in turbidites: an example from the Tertiary Piedmont Basin (Castagnola Fm., North Italy). Marine Petroleum Geology, Vol. 21 pp. 23-39.

Felletti, F., 2004b. Spatial variability of Hurst statistics in the Castagnola Formation, Tertiary Piedmont Basin, NW Italy: discrimination of sub-environments in a confined turbidite system. In: Confined Turbidite Systems (Eds L. Simon and J. Philippe). Special Publication of the Geological Society, Vol. 222, pp. 285-305, London.

Felletti, F**.,** Bersezio, R., 2010. Quantification of the degree of confinement of a turbidite-filled basin: a statistical approach based on bed thickness distribution. Marine and Petroleum Geology 27, 515-532.

Haughton, P.D.W., 1994. Deposits of deflected and ponded turbidity currents, Sorbas Basin, Southeast Spain. Journal of Sedimentary Research, Section A: Sedimentary Petrology and Processes 64(2): 233-246.

Haughton, P.D.W., 2000. Evolving turbidite systems on a deforming basin floor, Tabernas, SE Spain. Sedimentology 47(3): 497-518.

Haughton, P., Davis, C., McCaffrey, W., Barker, S., 2009. Hybrid sediment gravity flow deposits – Classification, origin and significance. Marine and Petroleum Geology 26, 1900–1918.

Hay, D.C., 2012. Stratigraphic Evolution of a Tortuous Corridor From The Stepped Slope of Angola, in: Prather, B.E., Deptuck, M.E., Mohrig, D.C., van Hoorn, B., Wynn, R.B. (Eds.), Application of the Principles of Seismic Geomorphology to Continental-Slope and Base-of-Slope Systems: Case Studies from Seafloor and Near-Seafloor Analogues. SEPM (Society for Sedimentary Geology), pp. 163-180.

Hickson, C. J. 2000. Physical controls and resulting morphological forms of the Quaternary ice-contact volcanoes in western Canada. Geomorphology, 32, 239-261.

Holman, W. E., & Robertson, S. S., 1994. Field development, depositional model and production performance of the turbiditic J sands at Prospect Bullwinkle, Green Canyon 65 field, outer shelf, Gulf of Mexico. In P. Weimer, A. H. Bouma, & B. F. Perkins (Eds.), Submarine fans and turbidite systems—sequence stratigraphy, reservoir architecture, and production characteristics (pp. 139–150). GCSSEPM Fifteenth Annual Research Conference.

Horine, R.L., Mills, W.H., Sturrock, V.J., and Anthony, M., 2000, Structural controls on sedimentation and hydrocarbon charge in the Troika Field—deepwater Gulf of Mexico (abstract):American Association of Petroleum Geologists, 2000 Annual Meeting, Abstract Volume,p. A69.

Kneller, B.C. and McCaffrey, W.D., 1999. Depositional effects of flow non uniformity and stratification within turbidity currents approaching a bounding slope; deflection, reflection, and facies variation. Journal of Sedimentary Research 69(5): 980-991.

Kneller, B.C., Edwards, D.A., McCaffrey, W.D., Moore, R., 1991. Oblique reflection of turbidity currents. Geology 19, 250-252.

Lamb, M.P., 2004. Surging versus continuous turbidity currents: Flow dynamics and deposits in an experimental intraslope minibasin. Journal of Sedimentary Research,74(1), 148-155. DOI: 10.1306/062103740148

Lamers, E., and Carmicheal, S.M.M., 1999, the Paleocene deepwater sandstone play, West of Shetland, *in* Fleet, A.J., and Boldy, S.A.R., eds., Petroleum Geology of Northwest Europe: Proceedings of the 5th Conference: Geological Society of London, p. 645–669.

Maino M., Decarlis A., Felletti F., Seno. S., 2013.Tectono-sedimentary evolution of the Tertiary Piedmont Basin (NW Italy) within the Oligo–Miocene central Mediterranean geodynamics. Tectonics, Vol. 32, pp.1–27, doi:10.1002/tect.20047.

Malinverno, A., 1997. On the power law size distribution of turbidite beds. Basin Res.9, 263–274.

Mosca P., Polino R, Rogledi S., Rossi M., 2010. New data for the kinematic interpretation of the Alps–Apennines junction (Northwestern Italy), Int J Earth Sci (Geol Rundsch), V. 99, pp 833–849.

McCaffrey, W.D., Kneller, B.C., 2001. Process controls on the development of stratigraphic trap potential on the margins of confined turbidite systems and aids to reservoir evaluation. American Association of Petroleum Geologists Bulletin 85, 1-18.

McGee, D.T., Bilinsky, P.W., Gary, P.S., Pfeiffer, D.S., and Sheman, J.L., 1994, geologic models and reservoir geometries of Auger Field, deepwater Gulf of Mexico, in Weimer, P., Bouma, A.H. and Perkins, B.F. eds., Submarine Fans and Turbidite Systems: SEPM Foundation, Gulf Coast Section, Fifteenth Annual Research Conference, p. 245–256.

Mahffie, M., 1993, Prospect Mars; Realization of Deepwater Potential in the Gulf of Mexico. Bulletin - Houston Geological Society, 36, 9.

Mahffie, M., M., 1995, Reservoir Classification for Turbidite Intervals at the Mars Discovery, Mississippi Canyon Block 807, Gulf of Mexico. Bulletin - Houston Geological Society, 37, 10.

Muck, M.T. and Underwood, M.B., 1990. Upslope flow of turbidity currents; a comparison among field observations, theory, and laboratory models. Geology (Boulder) 18(1): 54-57.

Mutti, E., Normark, W. R., 1991. An integrated approach to the study of turbidite systems. In: Weimer, P., Link, H. (Eds), Seismic Facies and Sedimentary Processes of Submarine Fans and Turbidite Systems. Springer-Verlag, pp. 75-106.

Ocean Drilling Project, 2004. ODP Logging Manual, Version 2.0. Available on line at: http://odplegacy.org/PDF/Operations/Science/Lab_Procedures/Cookbooks/Downhole/Logging_Manual.pdf

Patacci, M., Haughton, P. D. W. & McCaffrey, W. D, 2015. Flow behaviour of ponded turbidity currents. Journal of Sedimentary Research, in press.

Pickering, K.T. and Hiscott, R.N., 1985. Contained (reflected) turbidity currents from the Middle Ordovician Cloridorme Formation, Quebec, Canada; an alternative to the antidune hypothesis. Sedimentology 32(3): 373-394.

Pickering, K.T. & Hilton, V.C. 1998. Turbidite Systems of SE France. Vallis Press, London.

Prather, B.E., Booth, J.R., Steffens, G.S. and Craig, P.A., 1998. Classification, lithologic calibration, and stratigraphic succession of seismic facies of intraslope basins, deep-water Gulf of Mexico. AAPG Bulletin 82(5a): 701-728.

Prather, B.E., Pirmez, C., Winker, C.D., 2012. Stratigraphy of Linked Intraslope Basins: Brazos-Trinity System Western Gulf of Mexico, in: Prather, B.E., Deptuck, M.E., Mohrig, D.C., van Hoorn, B., Wynn, R.B. (Eds.), Application of the Principles of Seismic Geomorphology to Continental-Slope and Base-of-Slope Systems: Case Studies from Seafloor and Near-Seafloor Analogues. SEPM (Society for Sedimentary Geology), pp. 83-109.

Prather, B.E., Pirmez, C., Sylvester, Z. & Prather, D.S. (2012) Stratigraphic Response to Evolving Geomorphology in a Submarine Apron Perched on the Upper Niger Delta Slope. In: Application of the Principles of Seismic Geomorphology to Continental-Slope and Base-of-Slope Systems: Case Studies from Seafloor and near-Seafloor Analogues (Ed. by B. E. Prather, M. E. Deptuck, D. C. Mohrig, B. van Hoorn & R. B. Wynn), Sepm Special Publication 99, 145-161. SEPM (Society for Sedimentary Geology). "

Sinclair, H.D., 2000. Delta-fed turbidites infilling topographically complex basins; a new depositional model for the Annot Sandstones, SE France. Journal of Sedimentary Research 70(3): 504-519.

Sinclair, H.D., Cowie, P.A., 2003. Basin-floor topography and the scaling of turbidites.J. Geol. 111, 277–299.

Sinclair, H.D. and Tomasso, M., 2002. Depositional evolution of confined turbidite basins. *Journal of Sedimentary Research***72**(4): 451-456.

Smith, R. (2004). Silled sub-basins to connected tortuous corridors; sediment distribution systems on topographically complex sub-aqueous slopes. In: Lomas, S. A. and Joseph, P. (Eds). Confined Turbidite Systems. Geological Society of London Special Publication 222.

Smith, R., Joseph, P. 2004. Onlap stratal architectures in the Gres d'Annot; geometric models and controlling factors (in Deep-water sedimentation in the Alpine Basin of SE France; new perspectives on the Gres d'Annot and related systems) Geological Society Special Publications(2004), 221:389-399

Southern, S., Patacci, M., Felletti., F, and McCaffrey, W. 2015. On the influence of substrate entrainment and basin containment upon the development and depositional character of sandy hybrid event beds.

Stocchi, S., Cavalli, C., Baruffini, L., 1992. The Guaso (south-central Pyrenees), Gremiasco and Castagnola (eastern sector of Tertiary Piedmont basin) turbidite deposits:Geometry and detailed correlation pattern. Atti Ticinensi di Scienze della Terra, 35, 153-177.

Sylvester, Z., 2007. Turbidite bed thickness distributions: methods and pitfalls of analysis and modelling. Sedimentology 54, 847–870.

Sylvester, Z., Cantelli, A. and Pirmez, C. (2015). Stratigraphic evolution of intraslope minibasins: Insights from surface-based model. Aapg Bulletin 99(6): 1099-1129.

Talling, P.J., 2001. On the frequency distribution of turbidite thickness. Sedimentology 48, 1297–1331.

Talling, P.J., 2013. Hybrid submarine flows comprising turbidity current and cohesive debris flow: Deposits, theoretical and experimental analyses, and generalized models. Geosphere, 9(3), 460-488. DOI: 10.1130/GES00793.1

Tinterri, R., 2011. Combined flow sedimentary structures and the genetic link between sigmoidal- and hummocky-cross stratification. GeoActa, vol. 10, 2011, pp. 1-43.

Tomasso, M., 2001.Sedimentological evolution of topographically confined turbidite basins:The Annot Sandstones of southeast France [unpublished Ph.D. thesis]: The University ofBirmingham, 336 p.

Toniolo, H., Lamb, M. and Parker, G., 2006a. Depositional turbidity currents in diapiricminibasins on the continental slope: Formulation and theory. Journal of Sedimentary Research 76(5-6): 783-797.

Toniolo, H., Parker, G., Voller, V. and Beaubouef, R.T., 2006b. Depositional turbidity currents in diapiric minibasins on the continental slope: Experiments - Numerical simulation and upscaling. Journal of Sedimentary Research 76(5-6): 798-818.

Van Andel, T. and Komar, P.D., 1969. Ponded sediments of the Mid-Atlantic Ridge between 22o and 23o north latitude. Geological Society of America Bulletin 80: 1163-1190.

Winker, C.D., 1996. High-resolution seismic stratigraphy of a late Pleistocene submarine fan ponded by salt-withdrawal mini-basins on the Gulf of Mexico continental slope. Proceedings of the 28th annual Offshore Technology Conference, pp. 619-628.

Winker, C. D., & Booth, J. R., 2000. Sedimentary dynamics of the salt-dominated continental slope, Gulf of Mexico: Integration ofobservations from the seafloor, near surface, and deep subsurface. GCSSEPM Foundation 20th Annual Research Conference,1059–1086.

Castagnola Fm. members	basin size	dominant deposits	depositional style	interpretation
Mt. Brugi Marls Mb	unknown	bioturbated, marls and thin bedded turbidites	marly framework containing decameter-thick intercalations of laterally persistent thin bedded turbidites (a)	basin plain deposits (a)
Arenaceo Mb	unknown	thick bedded turbidites with high net/gross	lenticular, locally amalgamated turbidite beds with thin, laterally discontinuous mudstone partitions (a; b; c)	depositional lobes of a larger fan systems (a)
Costa Grande Mb	~ 6 km (SW-NE) X~ 4 km (NW-SE) (a, b)	thin to very thick bedded turbidites with low net/gross	sheet-like turbidites comprising thick, basin-wide mud caps (b, c)	deposition in a small confined basin (a, b)

Table 2

measurements	sampling interval thickness (cm)	approx. vertical resolution (cm)	routinely acquired
gamma ray	15	15	yes
neutron-density	3-10	20-60	yes
resistivity	15	60-200	yes
spontaneous potential	N/A, continuous	150-300	yes

density	2.5-15	40-50	yes
caliper	N/A, continuous	<0.1	yes
resistivity- formation microscanner	0.25	0.5	no

Table 3

bed type	thickness range (m)	sandstone basal grain size	description	interpretation	distribution
Type A	2-10	medium	normally graded beds with a lower crudely to planar-parallel laminated sandstone, a medial division with alternating massive-dewatered and planar-parallel laminated sandstones and an uppermost unit of silty sandstones with wavy and hummocky-like laminations. Mud caps are typically thicker than the underlying sandstone	deposition from large volume, possibly sustained turbidity currents ponded by the enclosing topography	Unit 1-2
Type B	0.5-4	fine-medium	normally graded beds comprising a thick lower division of parallel-laminated sandstone passing upward into silty sandstones with ripple drift cross-laminations consisting of multiple bedform sets with opposite paleocurrents. Mud caps are typically thicker than the underlying sandstone	deposition from turbidity currents of intermediate volume developing a ponded character in response to containment by the confining topography	Unit 1-2, and lower Unit 3

Type B'	0.4-1.6	medium-coarse	ungraded massive sandstone beds with sharp tops capped by very thin divisions of silty sandstones with ripple drift laminations. These beds can have scoured bases and be welded into amalgamated bed sets. Mud caps are a few cm to a few dm thick	rapid sedimentation from unconfined turbidity currents	Unit 3
Type C	0.6-3.5	medium-coarse	beds with a tripartite structure consisting of a lower massive sandstones and upper rippled sandstone sandwiching a poorly sorted muddy sandstone which can be charged with cm to dm-scale mud clasts or contain rafts of turbidite beds	deposition from hybrid flows, i.e. flows including the parent turbidity current and a co-genetic debris flow	ubiquitous
Type D	0.01-0.35	very fine	ripple-drift laminated sandstones grading upward into a mud cap which is typically few cm to several dm thick.	deposition from small volume, highly dilute waning flows	ubiquitous

Table 4

bed type	unit	number of beds	Mean	Standard deviation	Min	Median	Max	Skewedness
sandstone	1	33	1.98	2.3	0.4	1.04	10.4	2.37
beds	2	13	1,72	1.59	0.65	1.25	6.7	2.9
	3	87	0.94	0.5	0.05	0.9	3.2	1.25
mud caps	1	33	3.09	2.29	0.95	2.3	11.5	2.18
	2	13	1.21	0.33	0.75	1.21	1.85	0.42
	3	87	0.2	0.15	0.01	0.2	0.85	2.18

Figure 1

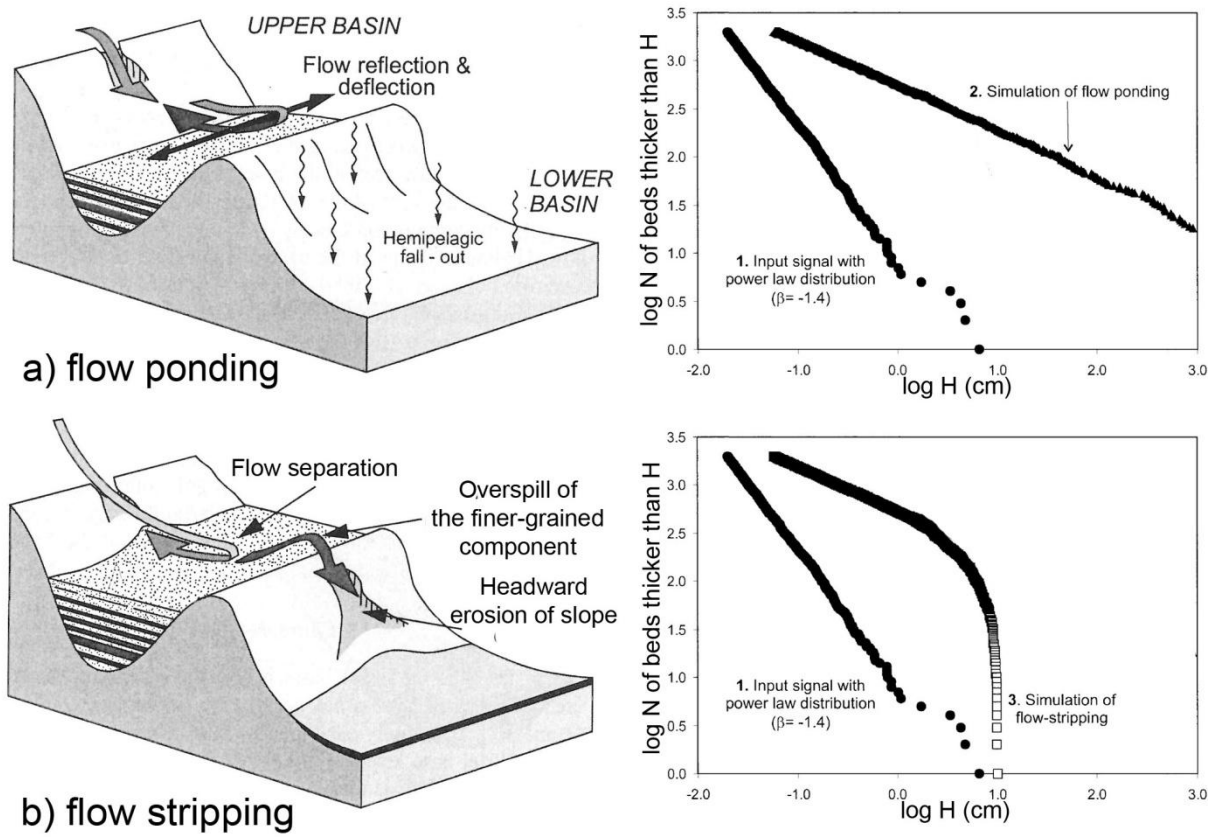

Figure 2

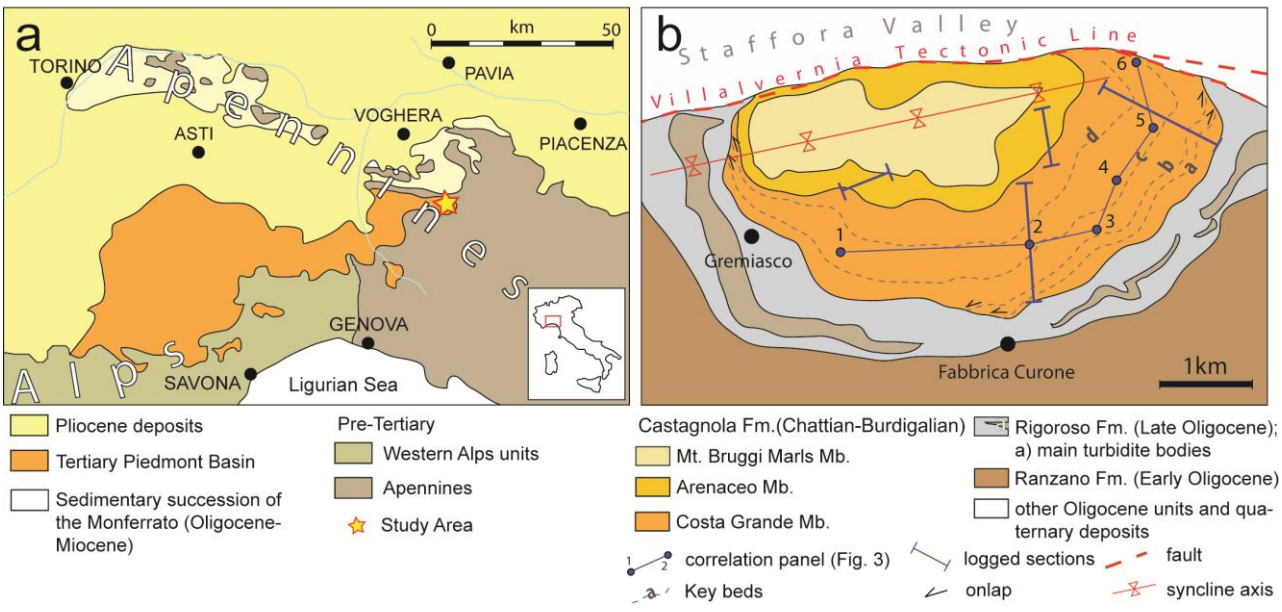

Figure 3

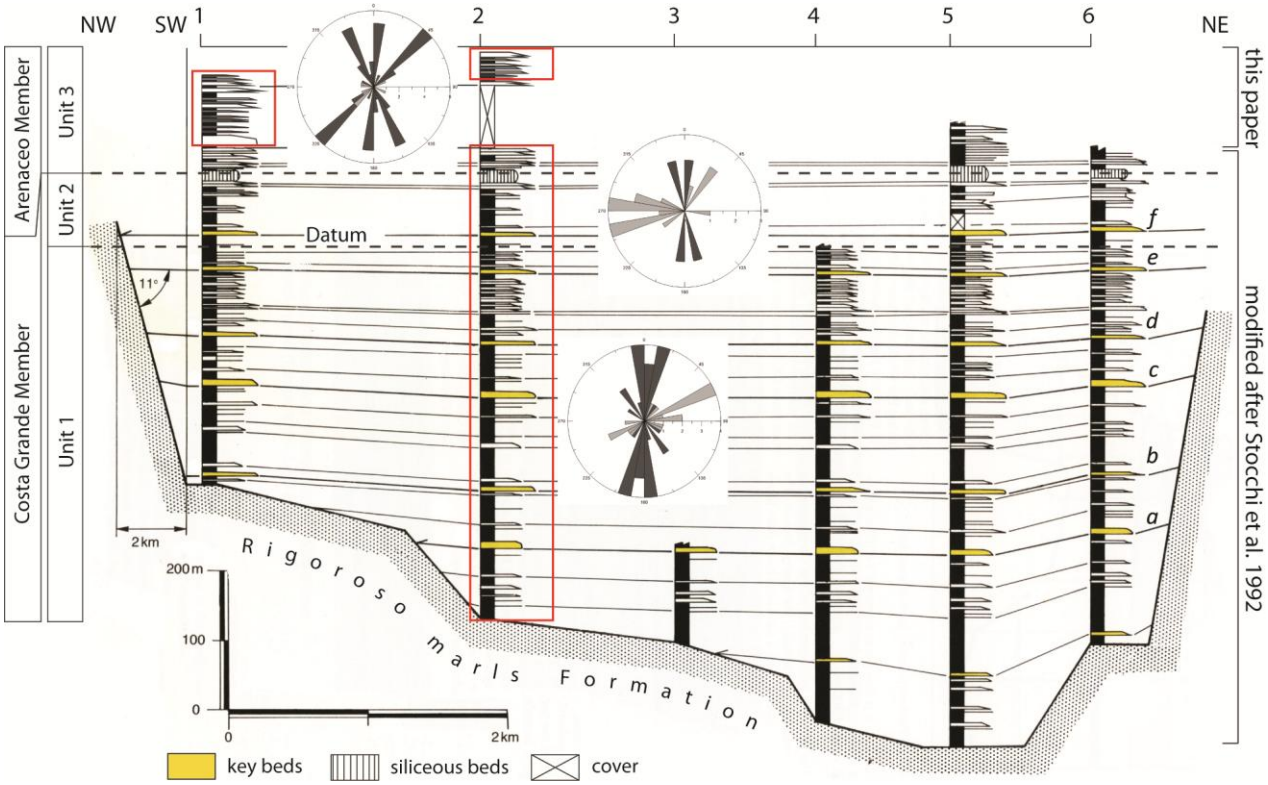
NW
SW
1
2
3
4
5
6
NE
this paper
modified after Stocchi et al. 1992
Arenaceo Member
Costa Grande Member
Unit 3
Unit 2
Unit 1
Datum
11°
2km
200m
100
0
0
2km
Rigoroso marls Formation
f
e
d
c
b
a
key beds
siliceous beds
cover

Figure 4

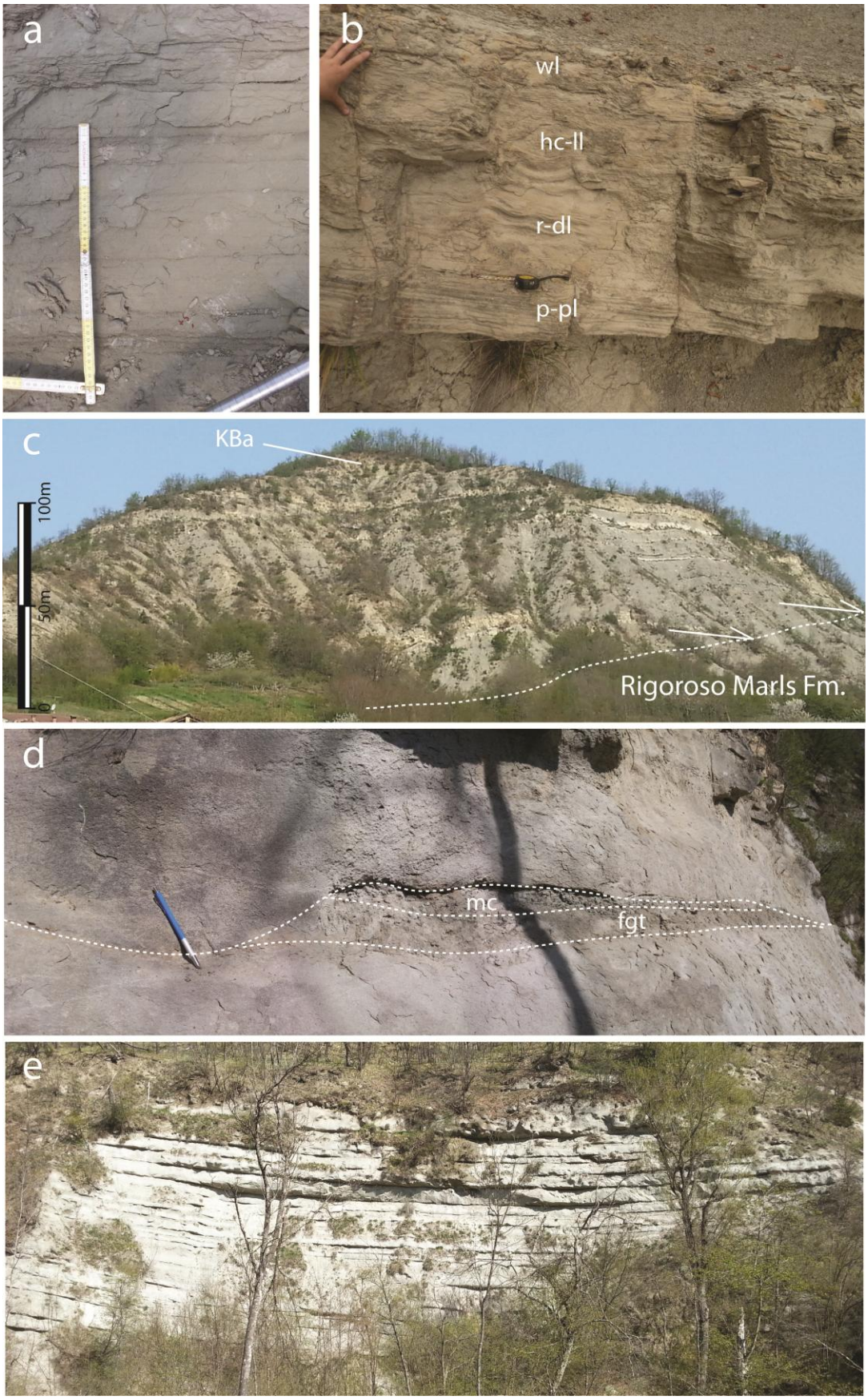

Figure 5

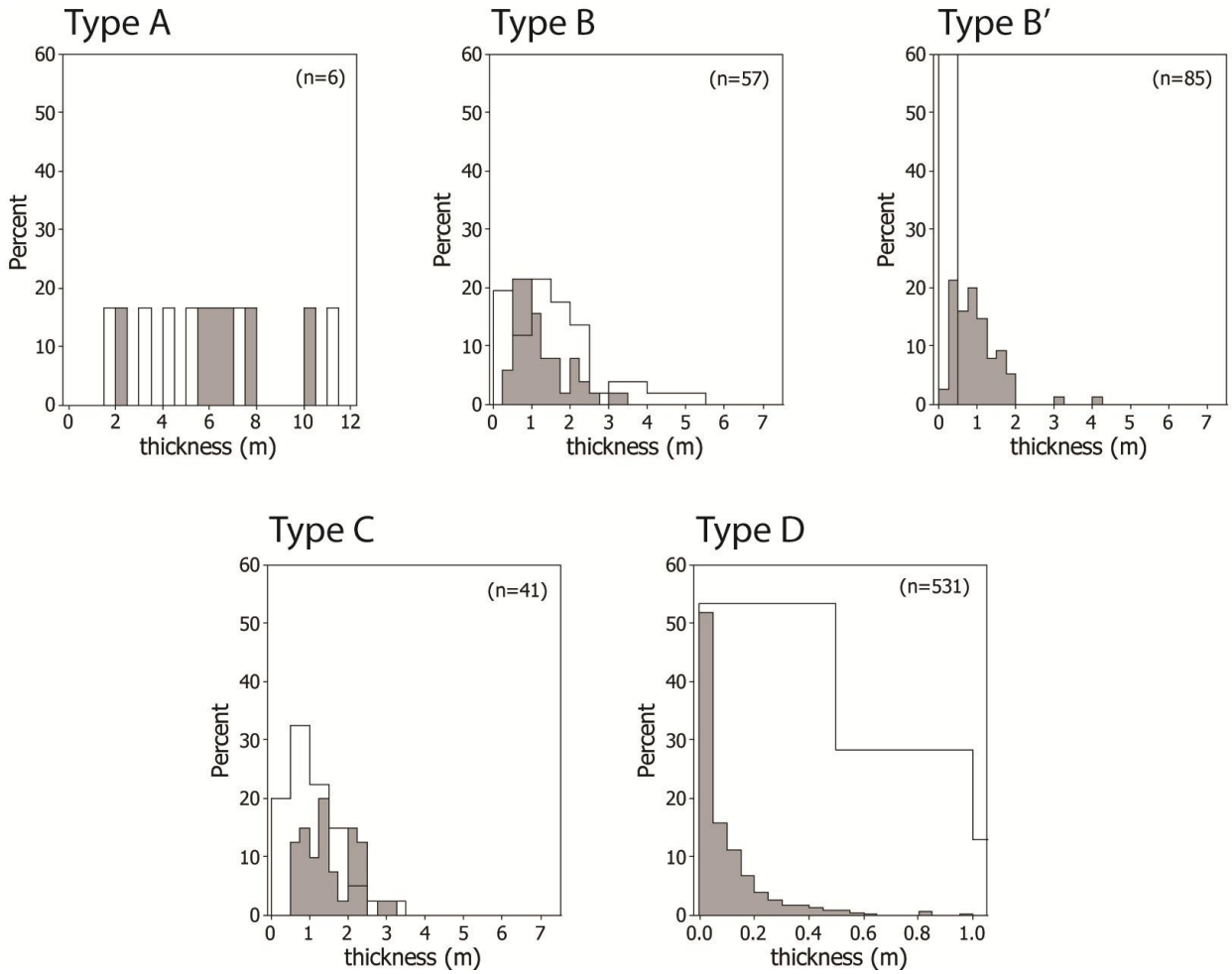
Type A
(n=6)
Percent
thickness (m)
Type B
(n=57)
Percent
thickness (m)
Type B′
(n=85)
Percent
thickness (m)
Type C
(n=41)
Percent
thickness (m)
Type D
(n=531)
Percent
thickness (m)

Figure 6

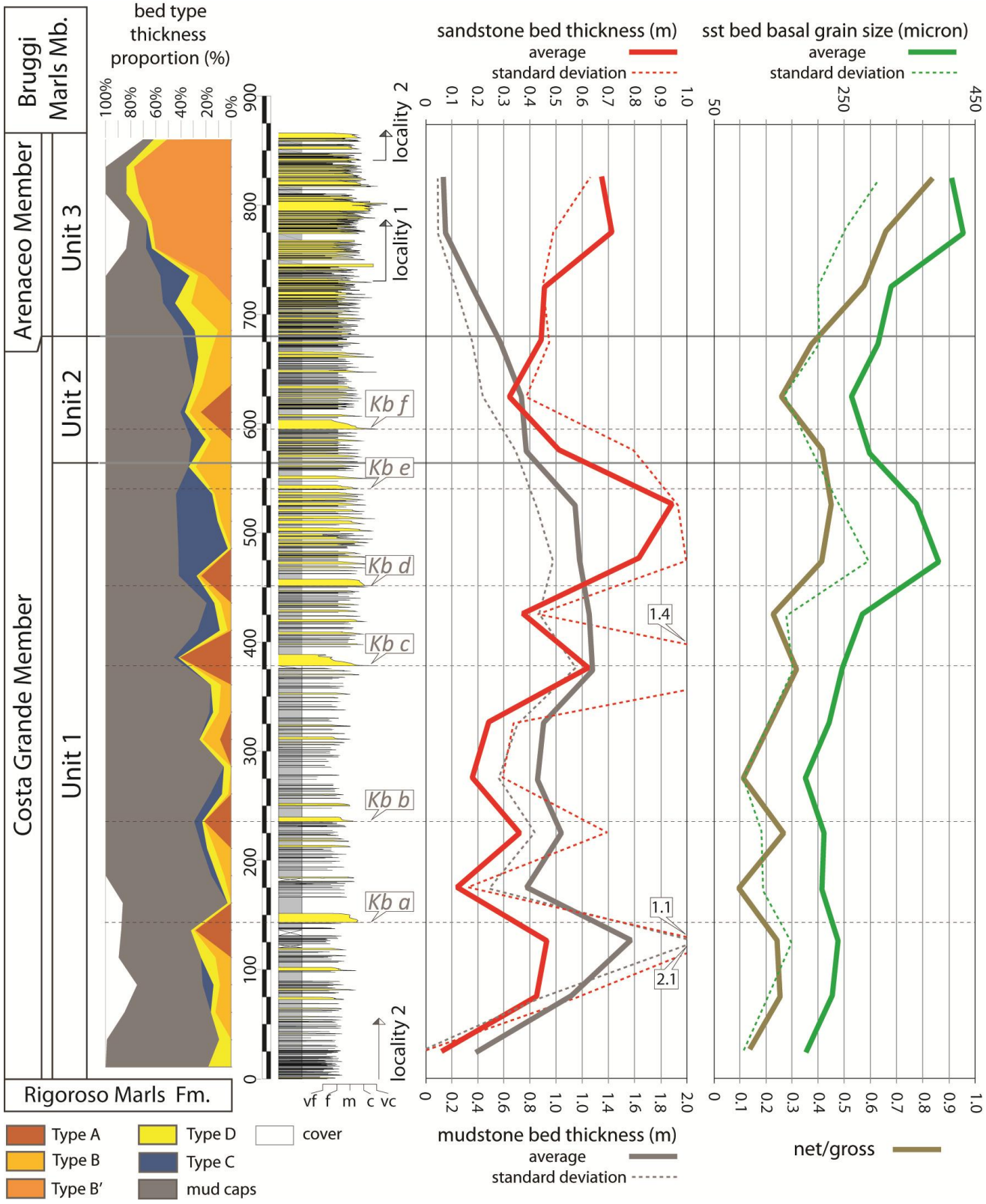
Bruggi Marls Mb.
Arenaceo Member
Unit 3
Unit 2
Unit 1
Costa Grande Member
Rigoroso Marls Fm.
bed type thickness proportion (%)
100%
80%
60%
40%
20%
0%
0
100
200
300
400
500
600
700
800
900
locality 2
locality 1
locality 2
Kb f
Kb e
Kb d
Kb c
Kb b
Kb a
vf f m c vc
sandstone bed thickness (m)
average
standard deviation
0 0.1 0.2 0.3 0.4 0.5 0.6 0.7 0.8 0.9 1.0
1.4
1.1
2.1
mudstone bed thickness (m)
average
standard deviation
0 0.2 0.4 0.6 0.8 1.0 1.0 1.4 1.6 1.8 2.0
sst bed basal grain size (micron)
average
standard deviation
50
250
450
net/gross
0 0.1 0.2 0.3 0.4 0.5 0.6 0.7 0.8 0.9 1.0
Type A
Type B
Type B'
Type D
Type C
mud caps
cover

Figure 7

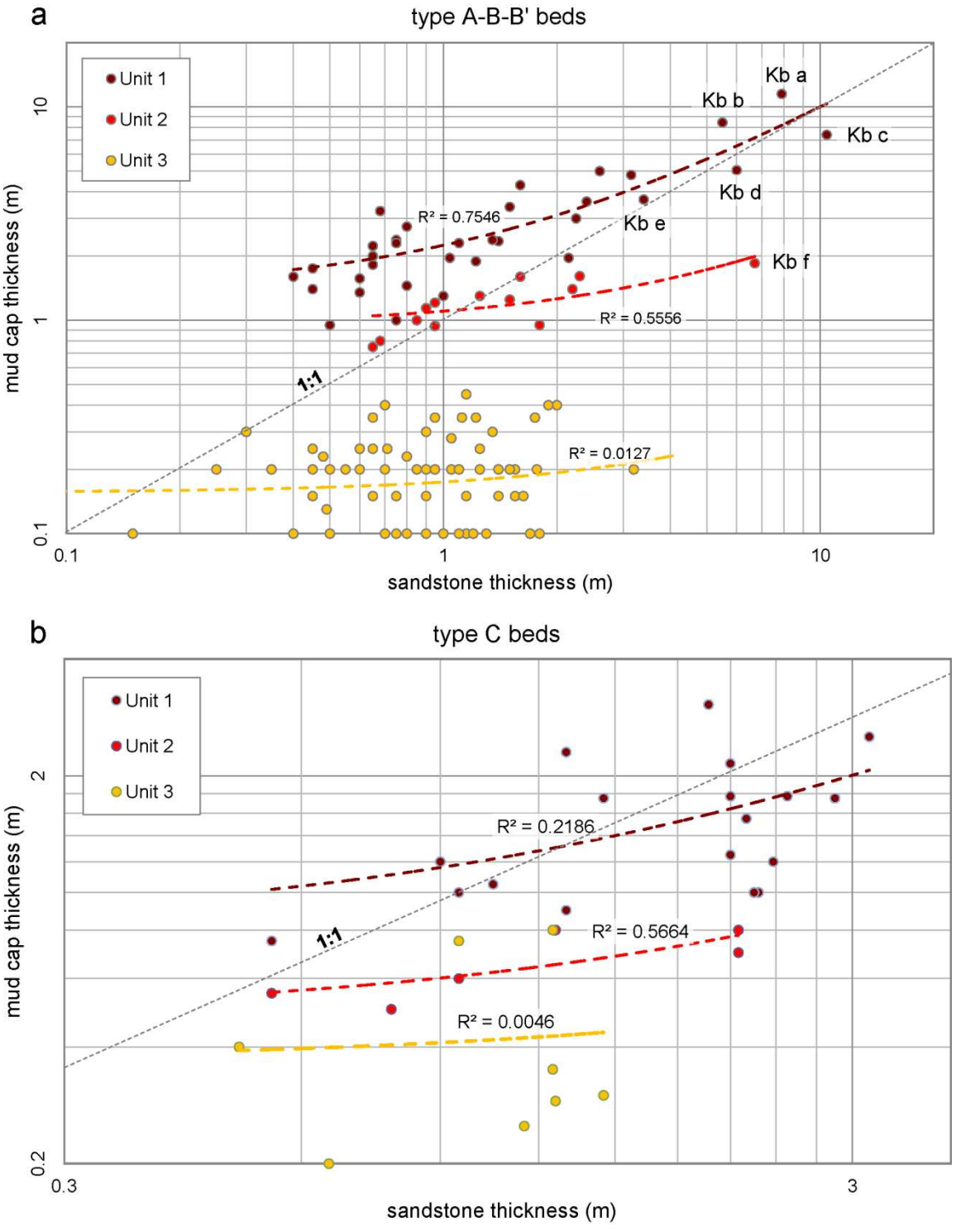
a
type A-B-B' beds
Unit 1
Unit 2
Unit 3
Kb a
Kb b
Kb c
Kb d
Kb e
Kb f
R² = 0.7546
R² = 0.5556
R² = 0.0127
1:1
mud cap thickness (m)
sandstone thickness (m)
0.1
1
10
b
type C beds
Unit 1
Unit 2
Unit 3
R² = 0.2186
R² = 0.5664
R² = 0.0046
1:1
mud cap thickness (m)
sandstone thickness (m)
0.2
2
0.3
3

Figure 8

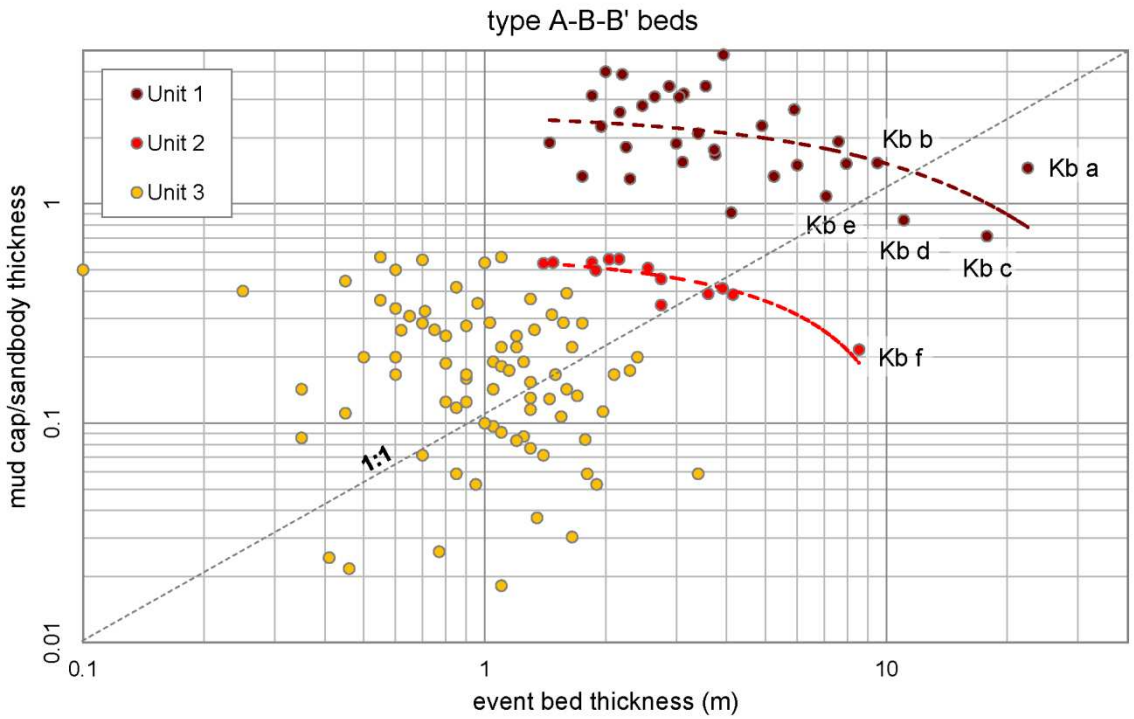

Figure 9

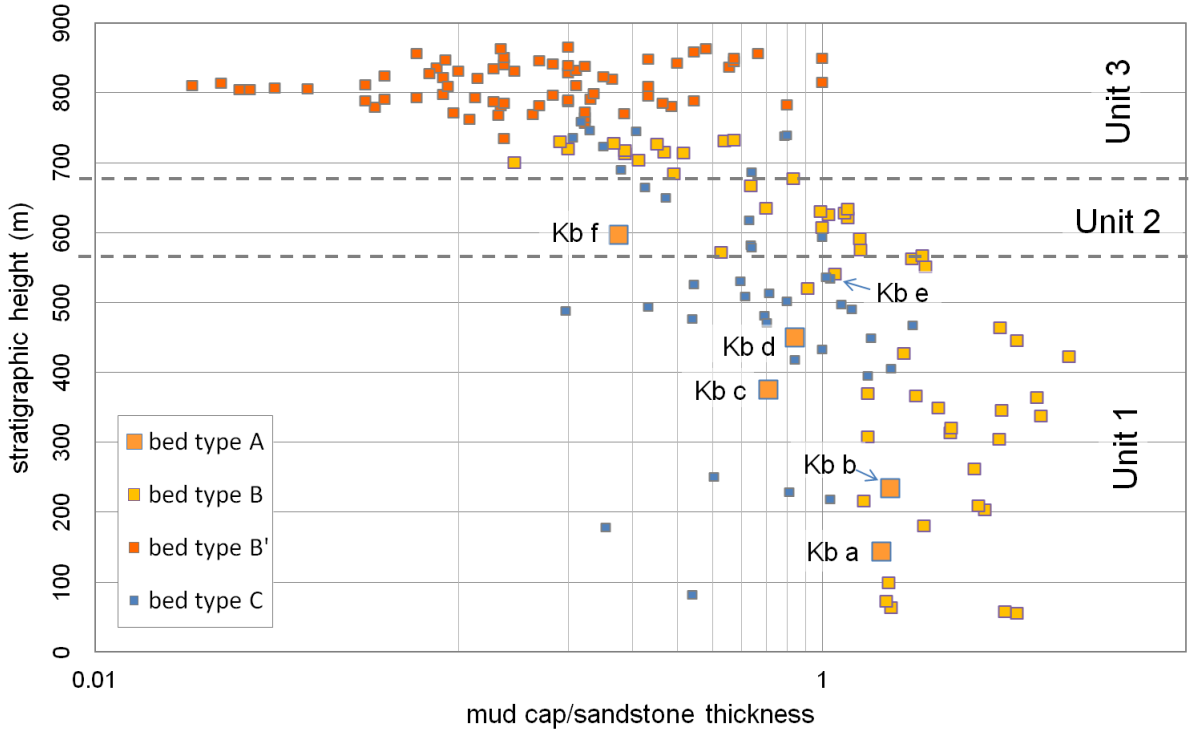

Figure 10

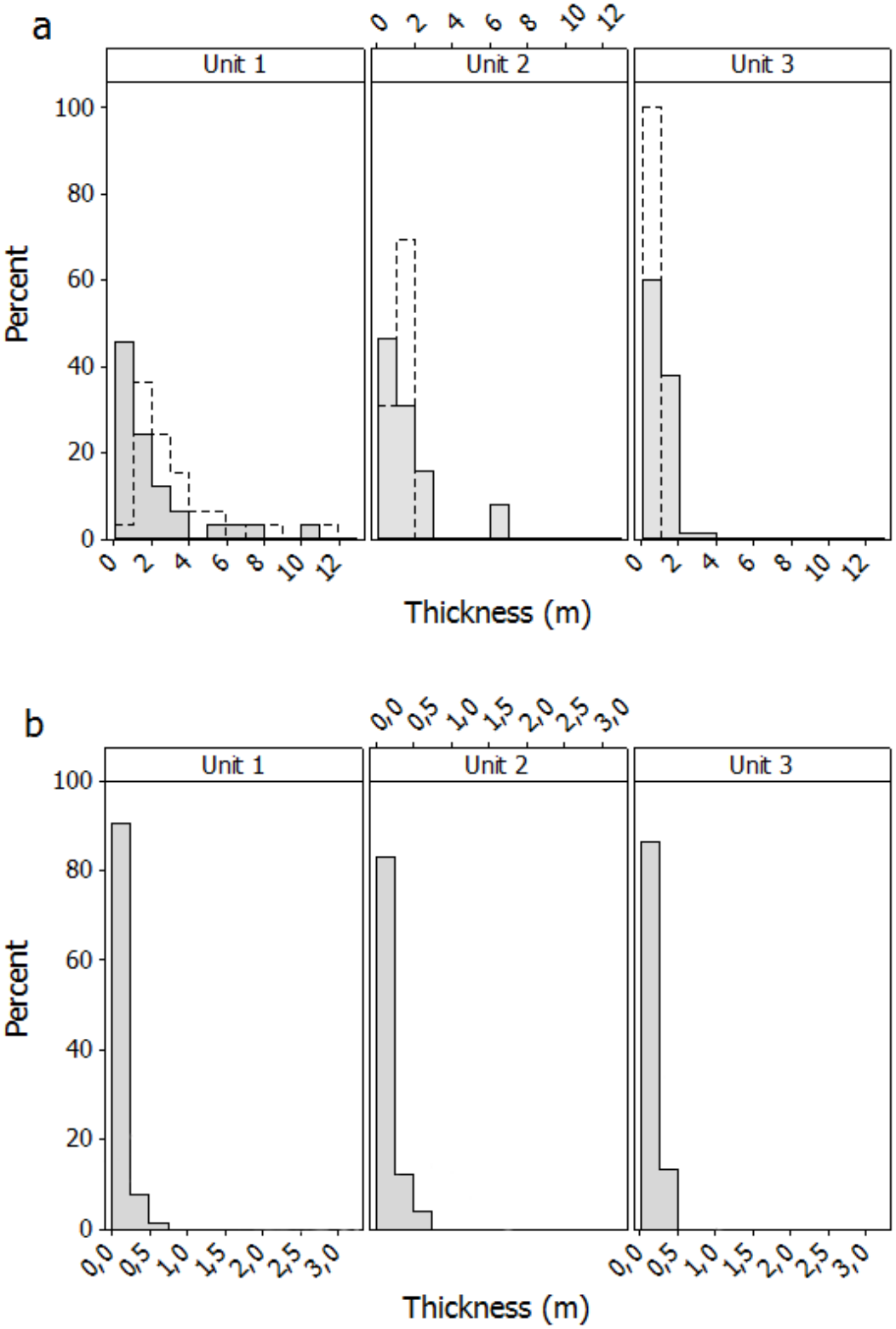
a
Unit 1
Unit 2
Unit 3
Percent
Thickness (m)
b
Unit 1
Unit 2
Unit 3
Percent
Thickness (m)

Figure 11

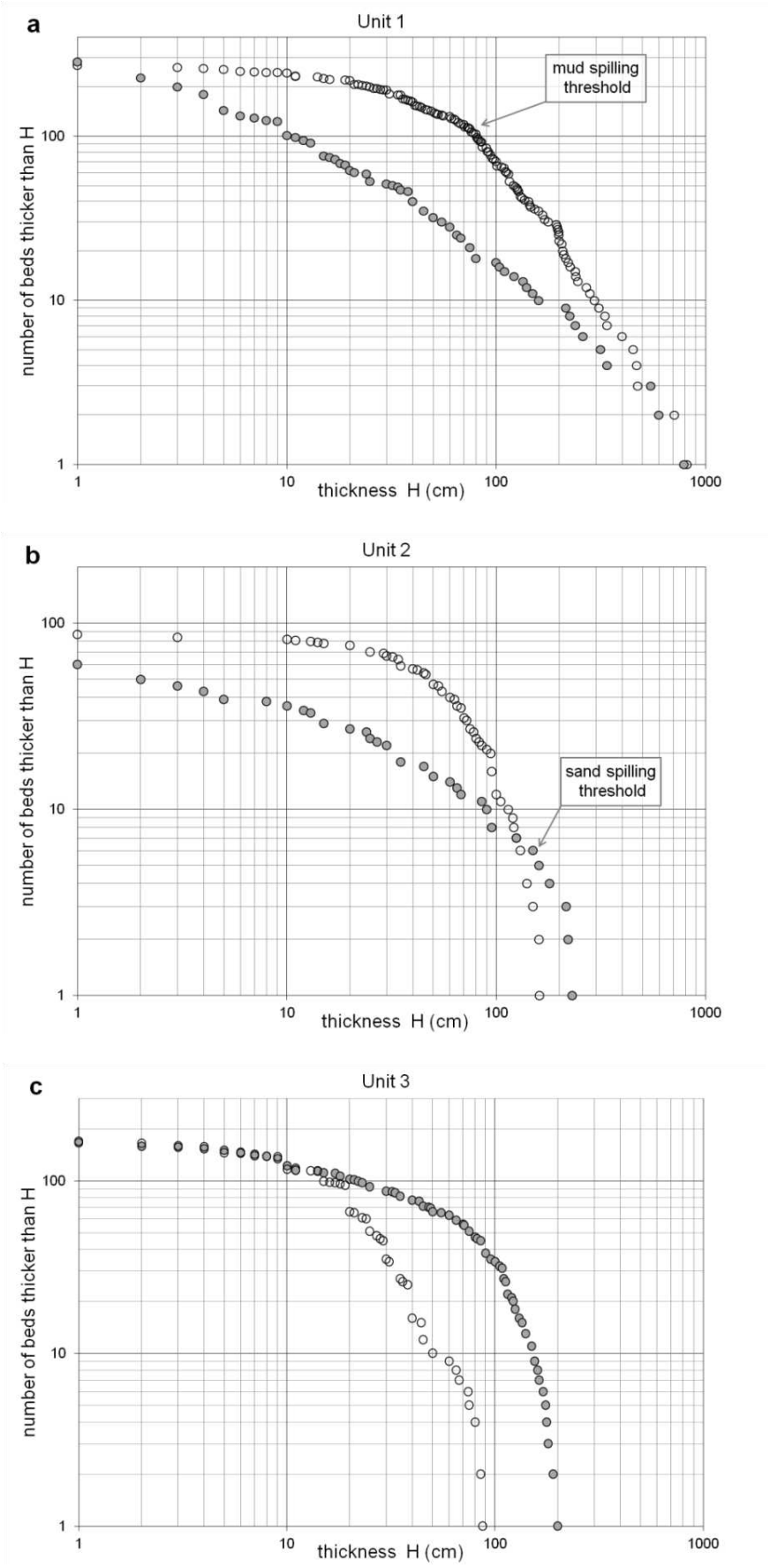
a
Unit 1
mud spilling threshold
number of beds thicker than H
100
10
1
1
10
100
1000
thickness H (cm)
b
Unit 2
sand spilling threshold
number of beds thicker than H
100
10
1
1
10
100
1000
thickness H (cm)
c
Unit 3
number of beds thicker than H
100
10
1
1
10
100
1000
thickness H (cm)

Figure 12

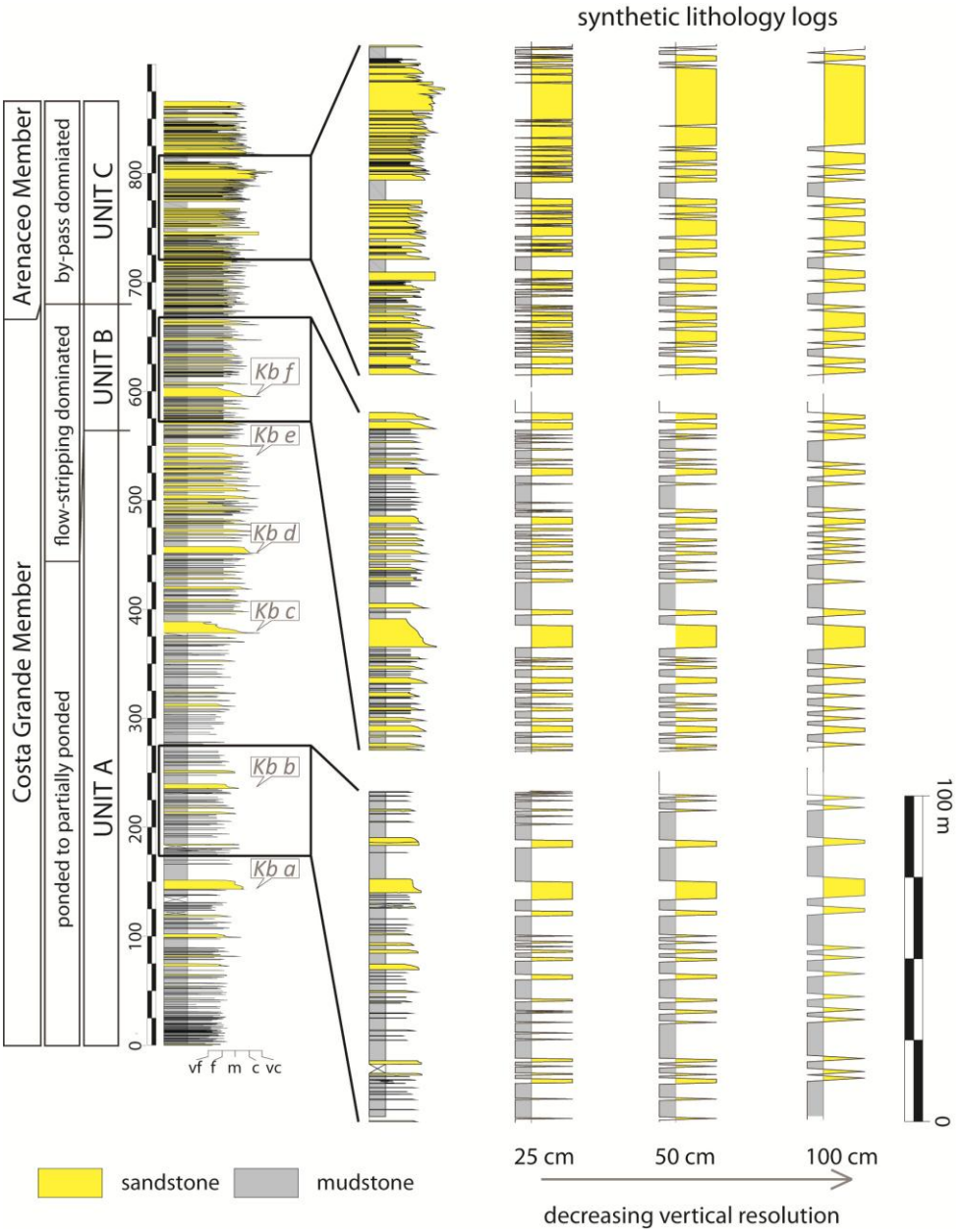
synthetic lithology logs
Arenaceo Member
Costa Grande Member
by-pass dominated
flow-stripping dominated
ponded to partially ponded
UNIT C
UNIT B
UNIT A
Kb f
Kb e
Kb d
Kb c
Kb b
Kb a
0
100
200
300
400
500
600
700
800
vf f m c vc
sandstone
mudstone
25 cm
50 cm
100 cm
decreasing vertical resolution
100 m
0

Figure 13

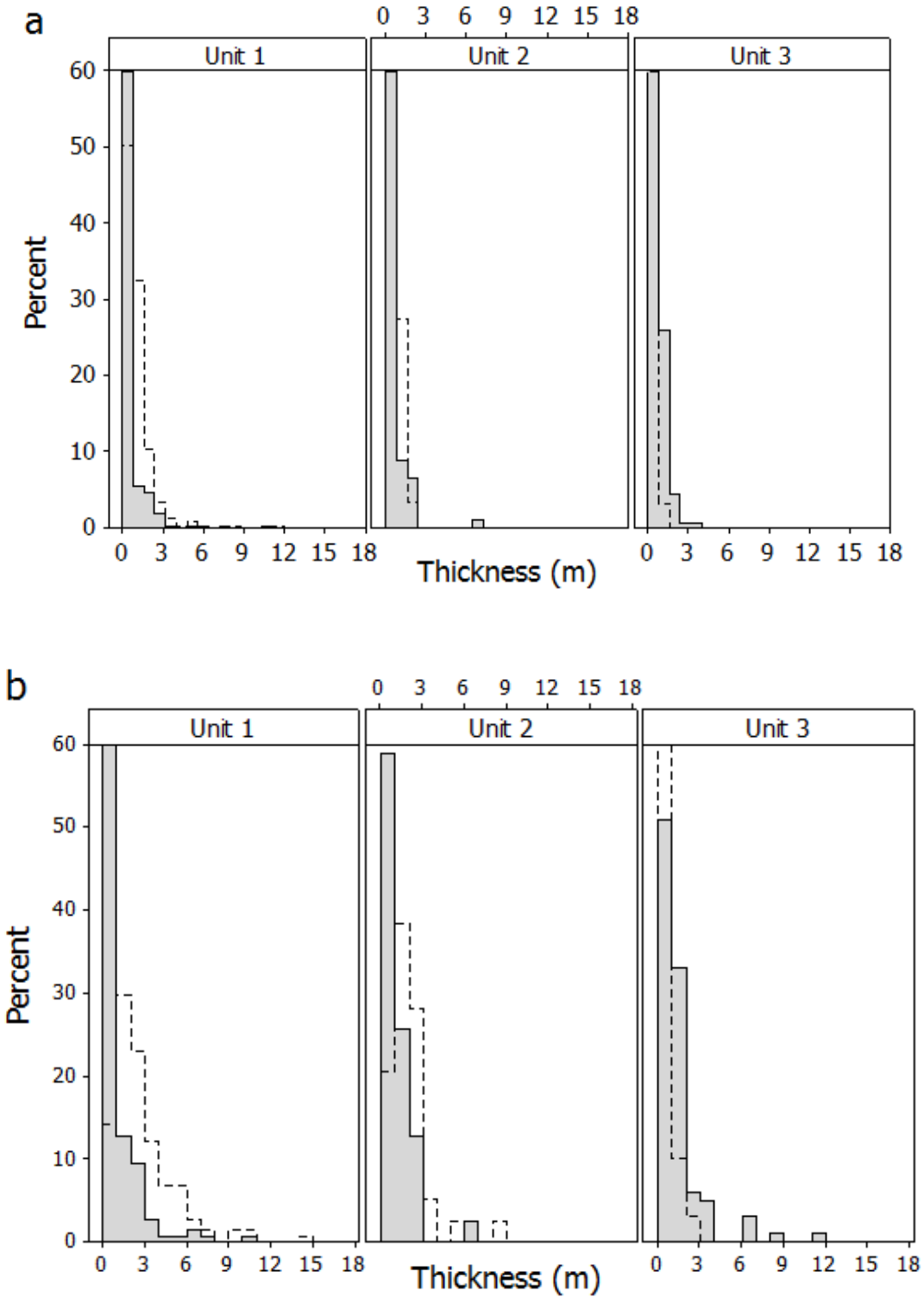
a
Unit 1
Unit 2
Unit 3
Percent
Thickness (m)
b
Unit 1
Unit 2
Unit 3
Percent
Thickness (m)

c

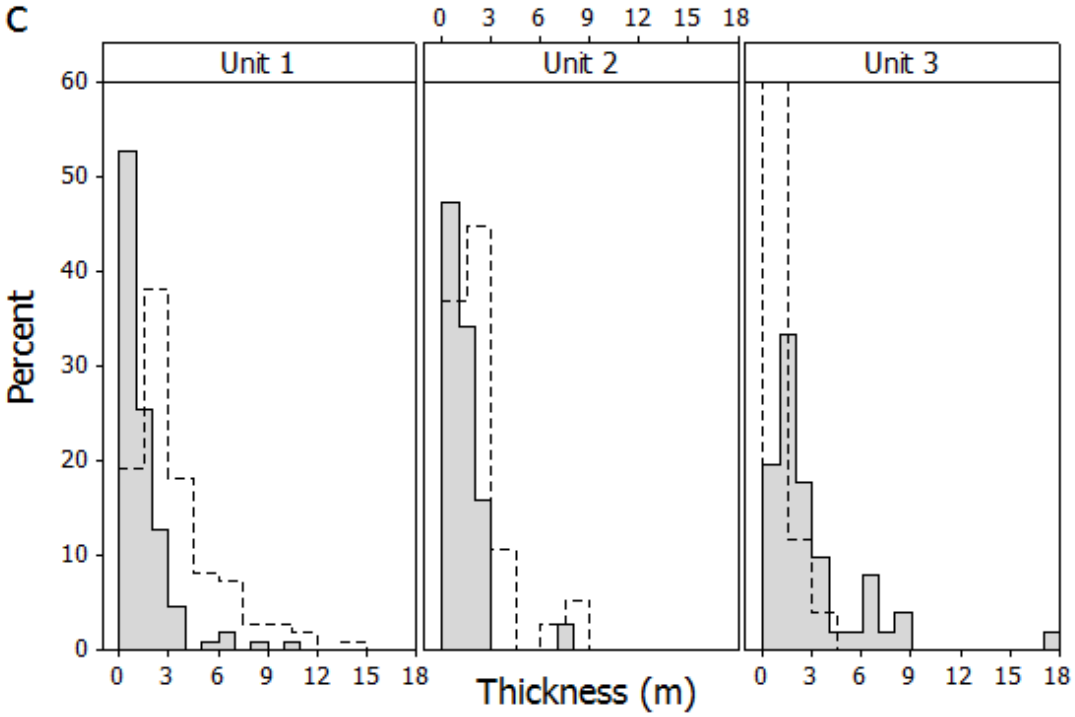
Unit 1
Unit 2
Unit 3
Percent
Thickness (m)
0 3 6 9 12 15 18
0 10 20 30 40 50 60

d

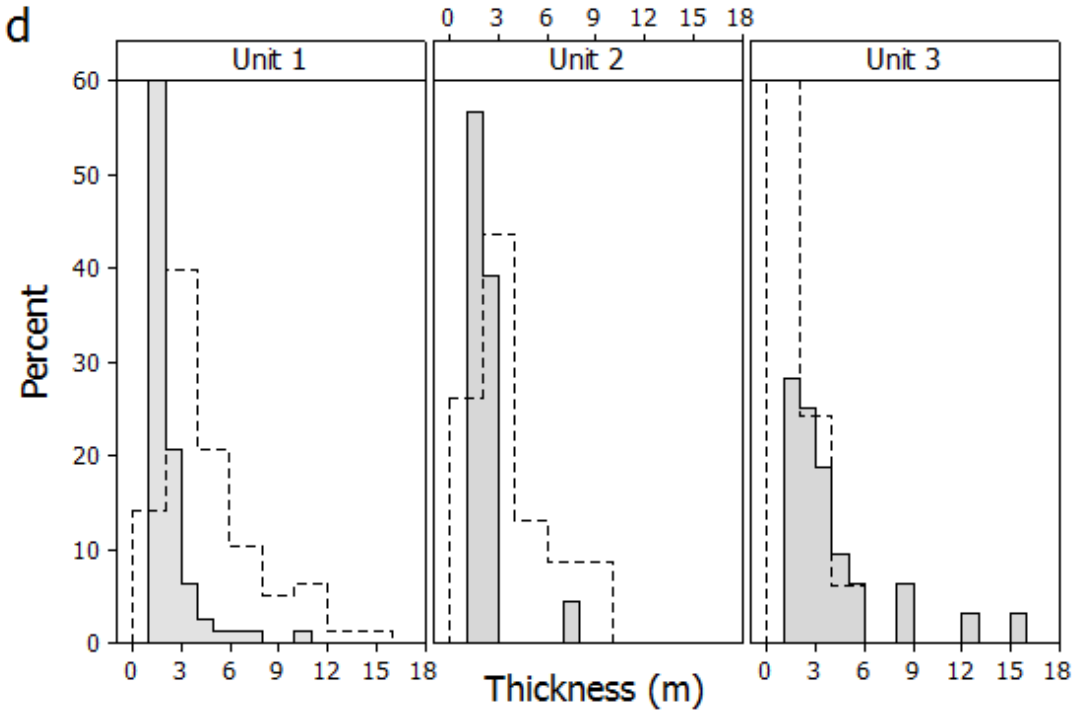
Unit 1
Unit 2
Unit 3
Percent
Thickness (m)
0 3 6 9 12 15 18
0 10 20 30 40 50 60

Figure 14

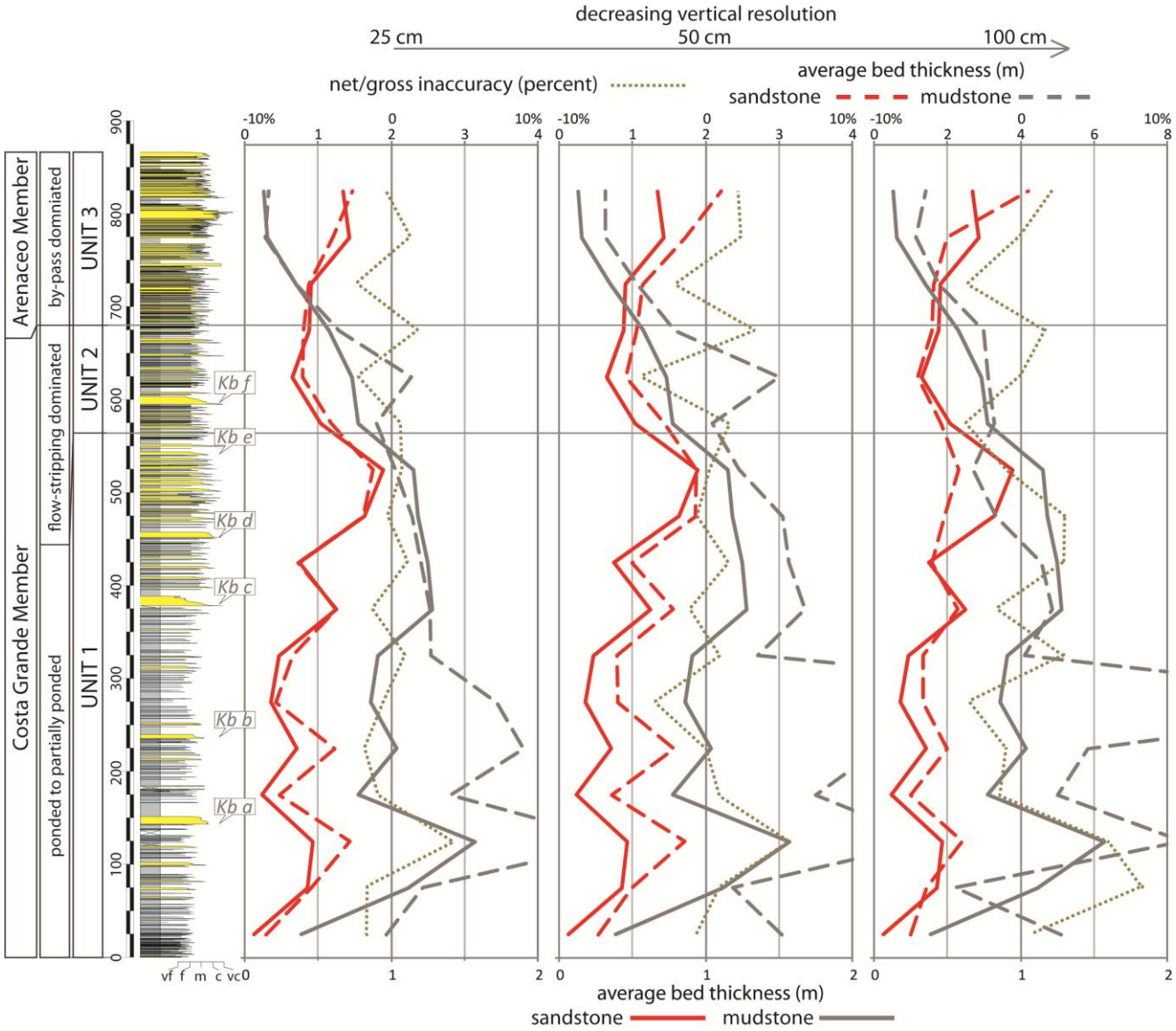
decreasing vertical resolution
25 cm
50 cm
100 cm
net/gross inaccuracy (percent)
average bed thickness (m)
sandstone
mudstone
Arenaceo Member
Costa Grande Member
by-pass dominated
flow-stripping dominated
ponded to partially ponded
UNIT 3
UNIT 2
UNIT 1
Kb f
Kb e
Kb d
Kb c
Kb b
Kb a
vf f m c vc
average bed thickness (m)
sandstone
mudstone